



HAL
open science

HssS activation by membrane heme defines a paradigm for 2-component system signaling in *Staphylococcus aureus*

Vincent Saillant, Léo Morey, Damien Lipuma, Pierre Boëton, Pascal Arnoux, Delphine Lechardeur

► To cite this version:

Vincent Saillant, Léo Morey, Damien Lipuma, Pierre Boëton, Pascal Arnoux, et al.. HssS activation by membrane heme defines a paradigm for 2-component system signaling in *Staphylococcus aureus*. 2023. hal-04184231

HAL Id: hal-04184231

<https://hal.science/hal-04184231>

Preprint submitted on 21 Aug 2023

HAL is a multi-disciplinary open access archive for the deposit and dissemination of scientific research documents, whether they are published or not. The documents may come from teaching and research institutions in France or abroad, or from public or private research centers.

L'archive ouverte pluridisciplinaire **HAL**, est destinée au dépôt et à la diffusion de documents scientifiques de niveau recherche, publiés ou non, émanant des établissements d'enseignement et de recherche français ou étrangers, des laboratoires publics ou privés.

1 **HssS activation by membrane heme defines a paradigm**
2 **for 2-component system signaling in *Staphylococcus aureus***

3 Vincent Saillant^a, Léo Morey^a, Damien Lipuma^a, Pierre Boëton^a, Pascal Arnoux^b and
4 Delphine Lechardeur^{a‡}

5 ^aMicalis Institute, INRAE, AgroParisTech, Université Paris-Saclay, 78350 Jouy-en-Josas,
6 France.

7 ^bAix Marseille Université, CEA, CNRS, BIAM, 13108, Saint Paul-Lez-Durance, France.

8

9 [‡]Address correspondence: delphine.lechardeur@inrae.fr

10

11

12 Key words: heme; *Staphylococcus aureus*; two-component system; virulence; membrane

13

14 Note: in this report, heme refers to iron protoporphyrin IX regardless of the iron redox state,

15 whereas hemin refers to ferric iron protoporphyrin IX.

16 **Abbreviations:**

17 AF: AlphaFold

18 β -gal: β -galactosidase

19 CDM: Chemically Defined Medium

20 ECD: Extracellular Domain

21 HAMP: Histidine kinases, Adenyl cyclases, Methyl-accepting proteins and Phosphatases

22 Hb: hemoglobin

23 HK: Histidine Kinase

24 HisKA: family A of histidine kinase

25 Hrt: Heme-regulated transport

26 HssS: Heme sensing system Sensor

27 HssR: Heme sensing system Regulator

28 HrtR: Heme-regulated transport Regulator

29 IM-HK: Intramembrane Histidine Kinase

30 OPM : Orientation of Proteins in Membranes

31 PDC: PhoQ-DcuS-CitA

32 RFU: Relative Fluorescence Unit

33 RLU: Relative Luminescence Unit

34 TCS: Two-Component System

35 TM: Transmembrane

36 WB: Western blot

37

38

39

40 **Abstract**

41 Strict management of intracellular heme pools, which are both toxic and beneficial, can be
42 crucial for bacterial survival during infection. The human pathogen *Staphylococcus aureus*
43 uses a two-component heme sensing system (HssRS), which counteracts environmental heme
44 toxicity by triggering expression of the efflux transporter HrtBA. The HssS heme sensor is a
45 HisKA-type histidine kinase, characterized as a membrane-bound homodimer containing an
46 extracellular sensor and a cytoplasmic conserved catalytic domain. To elucidate HssS heme
47 sensing mechanism, a structural simulation of the HssS dimer based on Alphafold2 was
48 docked with heme. In this model, heme is embedded in the membrane bilayer with its 2
49 protruding porphyrin propionates interacting with 2 conserved Arg94 and Arg163 that are
50 located extracellularly. Mutagenesis of these arginines and of 2 highly conserved
51 phenylalanines, Phe25 and Phe128, in the predicted hydrophobic heme binding pocket
52 abolished the ability of HssS to induce HrtBA synthesis. This study gives evidence that
53 exogenous heme interacts with HssS at the membrane/extracellular interface to initiate HssS
54 activation to induce HrtBA-mediated heme extrusion from the membrane. This “gatekeeper”
55 mechanism could limit intracellular diffusion of exogenous heme in *S. aureus*, and may serve
56 as a paradigm for how efflux transporters control detoxification of exogenous hydrophobic
57 stressors.

58

59 **Importance**

60 In the host blood, pathogenic bacteria are exposed to the red pigment heme that concentrates
61 in their lipid membranes, generating cytotoxicity. To overcome heme toxicity, *Staphylococcus*
62 *aureus* expresses a membrane sensor protein, HssS. Activation of HssS by heme triggers a
63 phosphorelay mechanism leading to the expression of a heme efflux system, HrtBA. This
64 detoxification system prevents intracellular accumulation of heme. Our structural and
65 functional data reveal a heme-binding hydrophobic cavity in HssS within the TM helices at
66 the interface with the extracellular domain. This structural pocket is important for the
67 function of HssS as a heme sensor. Our findings provide a new basis for the elucidation of
68 pathogen sensing mechanisms as a prerequisite to the discovery of inhibitors.

69

70

71 **Introduction**

72 *Staphylococcus aureus* is a Gram-positive opportunist bacterium that asymptotically
73 colonizes the skin and nostrils of nearly one-third of the human population (1). However, this
74 organism can breach defensive barriers in the compromised host to cause invasive diseases
75 such as endocarditis, toxic shock syndrome, osteomyelitis, and sepsis (1). Like most
76 pathogens, successful infection by *S. aureus* involves the production of numerous virulence
77 determinants including toxins, immune-modulatory factors, and exoenzymes, and requires
78 expression of factors that facilitate adaptation to the varied host environments (2-4).

79 Heme, an iron containing tetrapyrrole, is the bioactive cofactor of blood hemoglobin
80 (Hb) (5). The importance of heme resides in the unique properties of its iron center, including
81 the capacity to undergo electron transfer, perform acid-base reactions, and interact with
82 various coordinating ligands (5, 6). On the other hand, redox reactions of heme iron with
83 oxygen generate reactive oxygen species (ROS), which provoke damage to proteins, DNA
84 and lipids (5, 6). Since heme is hydrophobic and cytotoxic, its concentration and availability
85 must be tightly regulated.

86 In addition to utilizing heme as a nutrient iron source, *S. aureus* can employ both
87 endogenously synthesized and exogenously acquired heme as a respiratory cofactor (7-9).
88 Heme toxicity is offset in *S. aureus* by a conserved strategy for heme detoxification and
89 homeostasis involving a heme-regulated efflux pump (HrtBA; Heme-regulated transport).
90 HrtBA was also identified in *Enterococcus faecalis*, *Lactococcus lactis*, *Streptococcus*
91 *agalactiae*, *Bacillus anthracis*, and *Corynebacterium diphtheriae* (10-13). HrtB topology
92 classifies this permease as a MacB-like ABC transporter (14, 15). Rather than transporting
93 substrates across the membrane, MacB couples cytoplasmic ATP hydrolysis with
94 transmembrane conformational changes to extrude substrates from the periplasmic side or
95 from the lateral side of its transmembrane domains (TM) (15, 16). A heme-binding site was

Membrane heme activates HssS

96 recently identified in the outer leaflet of the HrtB dimer membrane domain from which heme
97 is excreted (17).

98 HrtBA expression in numerous Gram positive pathogens is managed by HssRS (Hss;
99 heme sensing system), a two-component system (TCS) (13, 18-20). HssS senses heme
100 presence in the environment and transduces the signal to HssR, the transcriptional regulator of
101 *hrtBA* (13, 19, 20). HssS is a prototypical HisKA histidine kinase with a short Nt cytoplasmic
102 domain, and two TM helices flanking a 133 amino acid (AA) extracellular domain (19). The
103 Ct cytoplasmic domain is organized in structurally conserved modules: the HAMP domain
104 (present in Histidine kinases, Adenylate cyclases, Methyl accepting proteins and
105 Phosphatases) connects the second TM to the dimerization and histidine phosphorylation
106 domains (HisKA). A catalytic and ATP-binding (HATPase c) domain lies at the carboxyl
107 terminus. Upon activation, HssS undergoes autophosphorylation of the His-249 residue and
108 subsequently transfers the phosphoryl group to the Asp-52 residue of the HssR response
109 regulator (19). As HssS is activated by environmental heme, it is assumed that the HK
110 extracellular domain (ECD) harbors the sensing function (21).

111 Here, we show that membrane heme, rather than extracellular heme, is the activating
112 signal for the transient activation of HssS in *S. aureus*. To identify a domain within HssS that
113 may participate in heme signal reception, we performed a structural simulation of the dimer
114 which was docked with heme. A single conserved hydrophobic structural domain (per
115 monomer) with 2 conserved anchoring arginines at the interface between the membrane and
116 the extracellular domain were predicted to accommodate heme. Based on this approach, we
117 performed targeted mutagenesis and identified pivotal residues required for HssS binding to
118 heme. Our work reveals a new mechanism of direct ligand sensing of a histidine kinase at the
119 membrane level. We conclude that membrane heme control of HssS combined with

Membrane heme activates HssS

120 membrane heme extrusion by HrtB constitute a defense system for bacteria when they are
121 exposed to lysed erythrocytes.

122

123 **Results**

124 ***hrtBA* induction is the readout for HssS activation**

125 Heme conditions leading to expression of *hrtBA* and *hssS* were assessed. For this, an *S.*
126 *aureus* HG001 $\Delta hssRS$ mutant was transformed with plasmid *phssRS*-HA, encoding HssR and
127 a C-terminal HA-tagged version of HssS (Table S1). Antibodies against HA and HrtB were
128 used for detection (Fig. 1A). Amounts of HrtB were increased in the presence of heme, as
129 reported in *S. aureus* (13), while HssS expression remained constant (Fig. 1A). Accordingly,
130 *hssRS* promoter activity, measured by β -gal expression from a P_{hssRS} -*lac* fusion (pP_{hssRS} -*lac*,
131 Table S1), was independent of heme concentration (Fig. 1B). In contrast, the P_{hrtBA} reporter
132 (pP_{hrtBA} -*lac*; Table S1) responded linearly with increasing concentrations of exogenously
133 supplied hemin (Fig. 1C). As P_{hrtBA} was specifically activated by constitutively expressed
134 HssRS TCS (Fig. 1D), these data establish P_{hrtBA} induction as a specific reporter of HssRS
135 heme sensing and signaling.

136

137 **HssS transient activation by hemin signals intracellular heme accumulation**

138 To get insights into the mechanism of heme sensing by HssS, we followed the kinetics of
139 HssS stimulation by heme in WT HG001 with the fluorescent reporter (pP_{hrtBA} -GFP) (Table
140 S1). Hemin addition led to a transient P_{hrtBA} response at the beginning of HG001 growth, with
141 a maximal response output within a few hours post heme addition (Fig. 2A). No fluorescence
142 was detected in the strain carrying the promoterless plasmid (data not shown). At toxic heme
143 concentrations, P_{hrtBA} induction kinetics seems to follow the growth delay and reaches highest
144 induction in the presence of 1 and 2.5 μ M heme (Fig. 2A). P_{hrtBA} induction phase was
145 followed by a marked drop in fluorescence, likely corresponding to termination of the P_{hrtBA}
146 induction phase (Fig. 2A). In stationary phase bacteria, fluorescence associated to pP_{hrtBA} -GFP
147 expression stabilized following induction by heme, confirming the transient activation by

Membrane heme activates HssS

148 HssS (Fig. S1A). Expression kinetics of GFP and HrtB correlated as shown on WB (Fig.
149 S1B).

150 Negative control of HisKA is provided by its phosphatase activity on the
151 phosphorylated regulator. The conserved catalytic histidine residue together with the adjacent
152 conserved threonine residue (HXXXT motif) is a key target for HisKA phosphatases (22, 23).
153 To evaluate the role of HssS phosphatase activity in its activation dynamics, the threonine
154 T253 was mutated to alanine in the plasmid *phssRS*-HA, P_{hrtBA} -*gfp* (pGFP(HssS)) to generate
155 pGFP(HssS T253A) (Table S1). HG001 $\Delta hssRS$ was then transformed with both plasmids and
156 response to heme was characterized. Higher fluorescence emission was observed in the strain
157 expressing the HssS T253A allele compared to the WT strain, but remained transient (Fig.
158 2B). This result illustrates the duality of HssS as a kinase and phosphatase at any time point in
159 response to its activation by heme.

160 To test the possibility that transient HssS activation was related to HrtBA-mediated
161 heme efflux, kinetics of GFP expression from P_{hrtBA} in $\Delta hrtBA$ and WT strains by subtoxic
162 heme concentrations were compared (Fig. 2C). GFP expression was also transient in the
163 $\Delta hrtBA$ strain, indicating that HrtBA expression did not explain transient HssS activation.
164 While P_{hrtBA} dynamics were similar in both strains, fluorescence emission reached higher
165 values in $\Delta hrtBA$ (Fig. 2C). We hypothesize that HssS activation intensity is correlated to the
166 intracellular accumulation of heme upon *hrtBA* deletion. To test this, heme accumulation was
167 visualized by the color of culture pellets from the $\Delta hrtBA$ mutant compared to the WT strain
168 exposed to hemin (Fig. S2A). Accordingly, the $\Delta hrtBA$ mutant accumulated about twice more
169 heme than did the WT as evaluated by the pyridine hemochrome assay (Fig. S2B). These
170 results show that intracellular heme pools impact HssS activation, raising the question of
171 where the heme-HssS interface is localized.

Membrane heme activates HssS

172 Replacing free hemin by Hb led to a fluorescence emission intensity that was more
173 than 5 times higher in the $\Delta hrtBA$ strain than in the WT strain (Fig. 2D). Interestingly, the
174 kinetics of GFP expression were modified in the presence of Hb compared to hemin. Slow
175 and continuous delivery of hemin from Hb compared to a fast and short delivery of free
176 hemin to the bacteria could provide an explanation to the observed distinct kinetics of GFP
177 expression and transient HssS activation. These results further correlate membrane HssS
178 activation with intracellular heme accumulation.

179 The documented role of HssS as the signal transmitter required for HrtBA expression
180 gives strong *in vivo* evidence that HssS activation involves the pool of *S. aureus*-associated
181 heme rather than exclusively extracellular heme as generally considered (18-20). However, as
182 exogenous heme is detectable extracellularly, in the membrane, and in the cytoplasm (10, 24,
183 25), we cannot discriminate which bacterial compartment drives HssS activation.

184

185 **Heme docking on a prediction model of HssS reveals a putative heme binding region at** 186 **the interface between membrane and extracellular domains.**

187 Attempts to identify specific AAs residues within HssS that may participate in heme signal
188 reception have been hampered by the lack of an experimental three-dimensional structure. We
189 relied on an *in silico* approach using HssS structure prediction by AlphaFold2 (AF2). Results
190 of AF2 inferencing generated a model with a mean predicted local distance difference test
191 (pLDDT) value of 88 (<https://alphafold.ebi.ac.uk/entry/A5IVE3>). This indicates a confident
192 prediction, according to guidelines set out on EMBL's AlphaFold Protein Structure Database,
193 available at <https://alphafold.ebi.ac.uk>. Dimer prediction was obtained with Alphafold
194 advanced
195 ([https://colab.research.google.com/github/sokrypton/ColabFold/blob/main/beta/AlphaFold2_a](https://colab.research.google.com/github/sokrypton/ColabFold/blob/main/beta/AlphaFold2_advanced.ipynb)
196 [dvanced.ipynb](https://colab.research.google.com/github/sokrypton/ColabFold/blob/main/beta/AlphaFold2_advanced.ipynb)) (Fig. 3A). The structural cytoplasmic domains of the AF2 model were

Membrane heme activates HssS

197 consistent with previously assigned domain predictions (based on InterProScan annotations)
198 as displayed by a prototypical HisKA (Fig 3A). The overall structure of HssS ECD is a mixed
199 α/β fold with a PDC (PhoQ-DcuS-CitA)-like structure topology (26) (Fig. 3B). The central
200 4-stranded antiparallel β -sheet is flanked by α -helices on either side; a long N-terminal α -
201 helix and a short C-terminal α -helix that both lie on the same side of the sheet (Fig. 3B). The
202 long N-terminal helix is initiated by TM helix α 1 (identified as residues [11-31] by
203 Orientation of Proteins in Membranes (OPM, <https://opm.phar.umich.edu/>) and then
204 participates in the mixed α/β fold of the PDC domain. A second TM helix (helix α 4)
205 (identified as residues [166-187]) allows the polypeptide chain to run in the intracellular space
206 toward the HAMP and the HisKA domains (Fig. 3B).

207 We then used the program AutoDock Vina (<https://ccsb.scripps.edu/>) to dock heme on
208 the surface of the HssS dimer. Docking used either the intracellular domains or the membrane
209 and extracellular domains (Fig. 3B and Fig. S3). Using the intracellular part of HssS, all the
210 docking solutions are above -8 kcal/mol and are scattered on the surface of the protein (Fig.
211 S3). On the contrary, using the ECDs, all the docked solutions are below -8 kcal/mol and fall
212 on two areas that are related by the two-fold symmetry of the dimer, therefore representing a
213 single binding site (Fig. 3B). This binding site located at the interface between the lipid
214 bilayer and the extracellular space and defined by 2 helices α 1 and α 4, together with an
215 internal loop within the ECD (Fig. 3B-D). This predicted heme binding site is apolar on most
216 of its surface, except for the top that is lined with positive and negative charges (Fig. 3D and
217 Fig. 3E). In the best docking solution (-10.1 kcal/mol), the two heme propionates would be
218 able to engage in a salt-bridge, one with the conserved Arg94, the other with the conserved
219 Arg163 (Fig. 3E and Fig. S4). Furthermore, heme is surrounded by a few highly conserved
220 hydrophobic residues (Phe25, Phe128, and Phe165 belonging to the second monomer
221 (Phe'165) being below 4Å from the porphyrin ring (Fig. 3E and Fig. S4). This position did

Membrane heme activates HssS

222 not reveal the usual AAs that coordinate heme such as histidine, methionine or tyrosine.
223 Docking of heme on *S. epidermidis* HssS structural AF2 prediction (which shares 64 %
224 identity with *S. aureus* HssS) identified the same binding position (data not shown).

225 We next used an *hssS* mutational approach to challenge the proposed model of HssS
226 heme recognition.

227 Conservation of the predicted heme binding domain is determinant for HssS activation

228 We first examined the importance of the 2 conserved arginines Arg94 and Arg163 in heme
229 docking to HssS by generating alanine substitutions in pGFP(HssS) (Table S1). The three
230 constructs pGFP(HssS), pGFP(HssS R94A) and pGFP(HssS R163A) (Table S1) were
231 established in the HG001 $\Delta hssRS$ mutant. Activation by heme of either HssS R94A or R163A
232 was strongly diminished compared to the WT histidine kinase as shown by the diminished
233 fluorescence kinetic response (Fig. 4A). While expression levels of HssS R94A, HssS R163A,
234 and WT HssS were similar, expression of HrtB was strongly decreased in HssS point mutants
235 (Fig. 4B). Accordingly, the 2 arginine HssS variant strains showed marked heme sensitivity
236 compared to native HssS-containing strain (Fig. 4C and Fig. S5A). We conclude that heme
237 sensing is strongly dependent on Arg64 and Arg163, giving support to their role in anchoring
238 heme as predicted by docking (Fig. 4).

239 We next tested the importance of the predicted hydrophobic environment of heme. We
240 choose phenylalanines, Phe25 and Phe128, which are predicted to be less than 4 Å from heme
241 and could be engaged in π - π interactions that stabilize heme (Fig. 3E). The HG001 $\Delta hssRS$
242 mutant carrying either the F25A or F128A HssS variant (pGFP(HssS F25A) or pGFP(HssS
243 F128A)) (Table S1) showed similar expression levels as the WT counterpart; however, both
244 variants were defective for heme signal transmission to P_{hrtBA} (Fig. 5A and B). Moreover, both
245 variants showed increased heme sensitivity (Fig. 5C and Fig. S5B). As per predictions,
246 Phe165, a conserved AA that is more distant from heme (Fig. 5D) and would only be able to

Membrane heme activates HssS

247 contribute to heme stabilization from the edge of its aromatic ring, had a lower impact on
248 HssS activation (Fig. 5D). We conclude that, analogous to Arg94 and Arg163A; Phe25,
249 Phe128 are required for heme sensing and HssS function.

250 Finally, we constructed an HssS variant with the four mutations Arg64, Arg163,
251 Phe25 and Phe128 (pGFP (HssS 4 mut.)) (Table S1), each of which is positioned at less than
252 4 Å from the porphyrin (Fig. 3E). Despite being expressed at WT levels, this variant was
253 inactive and failed to induce HrtB expression (Fig. 6A and B). As expected, heme sensitivity
254 of the strain expressing HssS 4 mut. was similar to that of the $\Delta hssRS$ strain in the presence of
255 hemin (Fig. 6C and Fig. S5C).

256 Since the HssS variants tested are stable as shown by their expression on WB, we
257 conclude that the predicted heme anchoring AAs and the integrity of the surrounding
258 hydrophobic environment are essential for triggering HssS activation. These results supports
259 the structural model of heme interaction with HssS and therefore question the role and
260 importance of extracellular domain (ECD) of HssS.

261

262 **HssS lacking the extracellular domain [42-151] is constitutively activated**

263 We examined the impact of removing most of the [35-168] domain of HssS corresponding to
264 the ECD on heme signal transduction. A truncated version of *hssS* was constructed (referred
265 to as pGFP(HssS Δ ECD)) (Table S1), and was established in HG001 $\Delta hssRS$. In this variant,
266 the ECD AAs comprising AAs [35-41] and [151-168] were conserved and fused to allow
267 membrane insertion and thus lacked Arg94 and Phe128 that are essential for heme sensing
268 (see above). Expression and membrane localization of HssS-HA Δ ECD were verified on WB
269 using an anti-HA antibody following cell fractionation (Fig. S6A). Expression of the ECD
270 variant compared to the full length protein was lower, possibly suggesting differences in
271 protein stability (Fig. S6A).

Membrane heme activates HssS

272 To investigate the impact of the ECD deletion on HssS activity, GFP expression from
273 pGFP(HssS) and pGFP(HssS Δ ECD) was followed in the absence or presence of 1 μ M heme
274 (Fig. 7 A and B). Remarkably, P_{*hrtBA*}-GFP was expressed constitutively and independently of
275 heme addition in the strain carrying pHssS Δ ECD (Fig. 7 A and B). However, while HrtB
276 expression was constitutive, its levels were lower than in the strain producing WT HssS (Fig.
277 7C and Fig. S6A). Interestingly, despite lower levels of HrtB in the strain expressing
278 HssS Δ ECD, the strain showed markedly improved fitness when challenged with 10 μ M heme
279 when compared to the isogenic strain expression HssS WT (Fig. S6 B and C). This
280 observation appears to indicate a fitness advantage during infection of bacteria carrying a
281 defective HssS protein, such that *hrtBA* is constitutively active.

282 We conclude that in the absence of ECD, HssS does not retain its capacity to be
283 stimulated by heme, but also appears to transmit a basal signal leading to *hrtBA* induction and
284 bacterial protection against heme. The HssS Δ ECD phenotype contrasts with that of the Δ *hssS*
285 strain, which fails to induce *hrtBA*. It is thus tempting to speculate that HssS Δ ECD maintains
286 the heme binding domain open to accommodate heme. Altogether, these data point out the
287 importance of the extracellular domain for HssS activation.

288

289 **Discussion**

290 Heme homeostasis in Gram positive bacteria is mainly achieved *via* heme efflux. In *S. aureus*,
291 the major heme efflux transporter HrtBA is controlled by HssRS (13, 18, 27). Our results give
292 strong support that the heme sensing function of the dimeric HK HssS is located in a
293 structural domain at the interface between the TM and extracellular domains. Thus,
294 membrane-attached rather than extracellular heme pools control HssS transient activation,
295 shedding new light on a detoxification mechanism of an abundant host molecule in a major
296 human pathogen *S. aureus*.

297 Four lines of evidence support the hydrophobic HssS interface as being required for
298 heme binding: 1- In depth *in silico* modelling predicted HssS protein structure and heme
299 binding candidate amino acids. In heme docking simulations, heme interacted with both
300 periplasmic and lipid-embedded amino acids. 2- Loss of functional HssS activity correlated
301 with directed mutagenesis of heme binding candidate amino acids, consistent with their
302 functional roles. Mutations of targeted AA in the hydrophobic environment and in predicted
303 anchoring arginines (Arg94 and Arg163), were all required to abolish HssS activation. 3- The
304 implicated amino acids and overall structure of *S. aureus* HssS are conserved in protein
305 homologs in other bacteria. These findings also clarify previous work in which random
306 mutations of conserved AA residues required for HssS heme sensing in *S. aureus* and in
307 *Bacillus anthracis* were mapped to the same domain (19, 20). 4- Heme availability from the
308 outside or from the inside lead to similar kinetics of induction. HssS is activated by
309 extracellular heme, but also by increasing intracellular heme pools (*e.g.*, in a $\Delta hrtBA$ mutant),
310 suggesting that both heme sources are accessible to HssS binding; by deduction, this common
311 site would need to be the membrane.

312 Our findings implicate heme bound to the HssS membrane-outer surface interface as
313 activation signal of HssS. We suggest that this mechanism of TCS activation may more

Membrane heme activates HssS

314 generally be a novel basis for hydrophobic molecule sensing. A previously reported class of
315 HKs called intramembrane histidine kinase (IM-HK) perceives its stimuli in the membrane,
316 but not directly (28-30). Instead, an N-terminal signal transfer region consisting of two
317 transmembrane helices presumably connects the IM-HKs with the regulated accessory
318 membrane proteins that function as the true sensors. For HKs that lack most of the sensory
319 domain in the ECD, cell envelope stress sensing has been directly linked to the ABC
320 transporter *via* TM-TM interactions (28-30). In contrast, an activation mechanism based on
321 direct physical interaction between HssS and HrtBA seems unlikely since P_{hrtBA} is induced in
322 an *hrtBA* deletion mutant. HssS is thus not activated similarly to IM-HK. We thus propose
323 HssS as a paradigm for signaling by organic molecules, as produced by the host, which are in
324 contact with the membrane-surface interface. Membrane input could be particularly relevant
325 for regulators of efflux transporters controlling exogenous substrates, including antibiotics
326 (31-33).

327 *In silico* simulation revealed the membrane-surface interface as the site of HssS
328 interaction with heme, but does not take into account the role of the flexible phospholipid
329 environment, which varies according to conditions and environmental lipids (34). Since
330 intramembrane heme concentrations impact HssS activation (as seen by testing HssS
331 induction in the $\Delta hrtBA$ mutant), it is highly likely that heme crosses the membrane to
332 activate HssS. Membrane lipid properties would then be expected to modulate HssS
333 activation. We are currently investigating the impact of altering phospholipid composition on
334 HssS expression to test this prediction.

335 Our findings that membrane heme activates HssS provides a functional link between
336 HssS and HrtBA. HrtB is a member of the MacB family of efflux pumps that is distinct from
337 other structurally characterized ABC transporters (35). The structural basis for heme efflux by
338 HrtB was recently solved in *Corynebacterium diphtheriae*: the HrtB dimer forms a heme

Membrane heme activates HssS

339 binding site in the outer leaflet of the membrane, which is laterally accessible to heme (17).
340 HssS would have the integral role as heme “gatekeeper” that controls exogenous heme pools
341 to prevent translocation within the membrane and into the cytosol (Fig. 8). Membrane heme
342 may either enter passively into the intracellular compartment or be effluxed by HrtB before
343 this step. This alternative model is compatible with our observations that exogenous excess
344 heme is internalized in *S. aureus* independently of the Isd heme import system in our
345 experimental conditions ((36) and data not shown).

346 Unlike *S. aureus*, *L. lactis* and *E. faecalis* control HrtBA expression using
347 intracytoplasmic TetR transcriptional regulators (HrtR in *L. lactis* (12) and FhtR in *E. faecalis*
348 (10)). It is thus tempting to speculate that possible that HssS sensing mechanism discriminates
349 heme originating from endogenous synthesis from exogenous sources, which would minimize
350 interference with metabolic processes.

351 *Staphylococcus aureus* is a serious threat to public health due to the rise of antibiotic
352 resistance in this organism. As such, many efforts are under way to develop therapies that
353 target essential host adaptive processes in *S. aureus*. Our findings provide a new basis for the
354 elucidation of pathogen sensing mechanisms as a prerequisite to the discovery of inhibitors.

355

356 **Materials and methods**

357 **Bacterial strains.** The strains and plasmids used in this work are listed in
358 supplemental Table S1. Plasmid constructions procedures are outlined in the supplemental
359 data. *Staphylococcus aureus* strain HG001, a derivative of the RN1 (NCT8325) strain with
360 restored *rhsU* (a positive activator of SigB) (37). HG001 Δ *hrtBA* and Δ *hrssS* mutants
361 construction are described in supplemental information section.

362 **Bacterial Growth Conditions and Media.** *Staphylococcus aureus* HG001 and
363 USA300 and their derivatives were grown as ON pre-cultures at 37°C in rich BHI liquid broth
364 (DIFCO) supplemented with 0.2 % glucose with aeration by shaking at 200 rpm. All growth
365 assays were performed in a 96-well plate in 200 μ l of BHI. Optical density at 600 nm (OD₆₀₀)
366 served as a measurement of growth and was measured every 15 min for the indicated total
367 time in a microplate reader (Spark, Tecan). *E. coli* strains were grown in Luria-Bertani (LB)
368 medium at 37°C with aeration by shaking at 180 rpm. When needed, antibiotics were used as
369 follows: 50 μ g/ml kanamycin and 100 μ g/ml ampicillin for *E. coli*; 5 μ g/ml erythromycin for
370 *S. aureus*. Hemin was prepared from a stock solution of 10 mM hemin chloride dissolved in
371 50 mM NaOH; Frontier Scientific).

372 **Dynamics of fluorescence emission.** For kinetic studies using GFP, *S. aureus* strains
373 were grown a 96-well plate in 200 μ l CDM (chemically defined medium) as reported (38, 39).
374 CDM medium contained around 170 nM iron (38). CDM is uncolored therefore minimizing
375 fluorescence background. OD₆₀₀ and fluorescence (Exc.: 480 nm; Em.: 515 nm, bandwidth: 9
376 nm, integration time: 40 μ s, gain: 140) were measured every 5 min in a black 96-well
377 microplate with transparent bottom (Greiner Bio-one, Kremsmünster, Austria) in a
378 spectrofluorimeter (Infinite M200, Tecan) at 37 °C under constant shaking (orbital,
379 amplitude: 2.5).

380 **Antibodies.** An anti-HrtB antibody targeted to the extracellular domain of *S. aureus*
381 HG001 HrtB was produced. The HrtB[45-236] fragment was purified from *E. coli* as a His-
382 tagged antigen from the plasmid pET200-*hrtB* ECL (see above and Table S1), purified from
383 bacterial lysates on a nickel affinity resin (His-Select, Sigma-Aldrich) as described (12).
384 Briefly, *E. coli* BL21 (DE3) (Thermo Fisher France, Villebon-sur-Yvette) transformed with
385 pET200-*hrtB* ECL was grown to $OD_{600} = 0.6$, and expression was induced with 1 mM
386 isopropyl 1-thio- β -D-galactopyranoside for 2 h at 37 °C. Cells were pelleted at $3,500 \times g$ for
387 10 min, resuspended in 50 mM Tris-HCl, pH 8.0, 300 mM NaCl, containing 20 mM imidazole
388 (binding buffer), and disrupted with glass beads (Fastprep, MP Biomedicals France, Illkirch-
389 Graffenstaden). Cell debris were removed by centrifugation at $18,000 \times g$ for 15 min at 4 °C.
390 The soluble fraction (supernatant) was mixed with the nickel affinity resin and incubated on
391 a spinning wheel at 4°C for 1 h. The resin was then centrifuged (5000 rpm, 5 min) and
392 washed three times with binding buffer. Purified proteins were eluted with 50 mM Tris-HCl,
393 pH 8.0, 300 mM NaCl, containing 150 mM imidazole, dialyzed against 50 mM Tris-HCl, pH
394 7.5, and finally stored at -80 °C. Protein concentrations were determined with the Lowry
395 assay method (Bio-Rad France, Marnes-la-Coquette). The resulting purified His-HrtB-ECL
396 was used for rabbit antibody production (Covalab, Bron, France). Antiserum specificity was
397 determined by Western blots using known amounts of purified His-HrtB-ECL proteins and
398 bacterial lysates expressing HrtB. The polyclonal anti-GAPDH antibody was a generous gift
399 from F. Götz (University of Tübingen, Germany) (40). The polyclonal anti-HA antibody was
400 from Thermo Fisher.

401 **Bacterial lysate and membrane isolation.** Bacteria were pelleted by
402 centrifugation and washed with PBS. Resuspended cells were then pelleted at 3,500 g for 10
403 min, resuspended in 50 mM Tris-HCl pH 7.5, 150 mM NaCl, containing 0.2% Triton (lysis
404 buffer), and disrupted with glass beads (Fastprep; MP Biomedicals). Cell debris were

Membrane heme activates HssS

405 removed by centrifugation at 18,000 *g* for 15 min at 4°C. To prepare membranes, bacterial
406 lysates were prepared as above except that bacteria were lysed in 20 mM Tris-HCl pH 7.5.
407 Lysates were then submitted to centrifugation at 100,000 *g* for 45 min at 4°C in an
408 Ultracentrifuge Beckman XL-90 (Beckman France, Villepinte) equipped with a 70.1T1 rotor.
409 Membranes pellets were resuspended in lysis buffer. Proteins were quantified by the Lowry
410 Method (Bio-Rad) and denatured in Laemmli sample buffer at 95°C for 5 min.

411 **β-galactosidase assays.** β-galactosidase activity was quantified by luminescence in an
412 Infinite M200 spectroluminometer (Tecan) using the luminescence β-glo assay as recommended
413 by the manufacturer (Promega France, Charbonnières-les-Bains, France). Briefly, *S. aureus*
414 strains cultures were diluted from ON precultures in BHI to an OD₆₀₀ = 0.01 and grown to an
415 OD₆₀₀ = 0.5 and then incubated for 1 h with the indicated concentrations of hemin. 25 μl
416 cultures were distributed in a white 96-wells microplate (Greiner Bio-one) in triplicate. 50 μl
417 β-glo assay reagent was added per well. After 10 min incubation at RT, luminescence was
418 quantified. In parallel, 200 μl of the corresponding cultures were distributed in a transparent
419 96-wells plate to measure the OD₆₀₀ for normalization of the luminescence.

420 **Heme concentration determination in bacterial lysates.** Proteins from bacterial
421 lysates (as described above) (in a volume of 250 μl) were mixed with 20 μl of 0.2 M NaOH,
422 40 % (v/v) pyridine and 500 μl potassium ferricyanide or 5 mM sodium dithionite. 500-600
423 nm absorption spectra were recorded in a UV-visible spectrophotometer Libra S22
424 (Biochrom, Cambridge,UK). Dithionite-reduced minus ferricyanide-oxidized spectra of
425 pyridine hemochromes were used to determine the amount of heme *b* by following the value
426 of the difference between absorbance at 557 nm (reduced) and 540 nm (oxidized) using a
427 difference extinction coefficient of 23.98 nM⁻¹.cm⁻¹ (41).

428 **Heme docking analysis.** Heme (<https://www.rcsb.org/>) was docked onto the modeled
429 HssS structure with AutoDock Vina 1.1.2 (<https://ccsb.scripps.edu/>). The exhaustivity

Membrane heme activates HssS

430 parameter was set to 8. Ligand and protein coordinates were prepared (including polar
431 hydrogen atoms and atoms charges to take hydrogen and electrostatic interactions into
432 account) using Open babel (http://openbabel.org/wiki/Main_Page). Docking of heme was
433 performed on the entire surface of one monomer in the dimeric HssS with 100 boxes (27.10^3
434 m^3). From each box, the top scoring pose (in terms of binding free energy (kcal/mol) as
435 estimated by AutoDock Vina) was selected for binding site. The 10 top docking solutions
436 were visualized with VMD ((42), <http://www.ks.uiuc.edu/Research/vmd/>) and designated a
437 single periplasmic.
438

439 **Acknowledgments.** This work was supported by the HemeDetox - 17-CE11-0044-01
440 project by the French “Agence Nationale de la Recherche”. V. Saillant is the recipient of a
441 doctoral fellowship from the French ministry of Research and Paris-Saclay University. The
442 funders had no role in study design, data collection and analysis, decision to publish, or
443 preparation of the manuscript. The funders had no role in study design, data collection and
444 analysis, decision to publish, or preparation of the manuscript. We thank Dr. A. Gruss
445 (INRAE, France) and Dr. P. Delepelaire (IBPC, France) for their technical help and insightful
446 comments on our work. We are grateful to A. Hiron (Université de Tours, France) and T.
447 Msadek (Institut Pasteur, France) for the HG001 $\Delta hssRS$ *Staphylococcus aureus* strain and to
448 Dr. F. Götz (University of Tübingen, Germany) for the generous gift of the anti-GAPDH
449 antibody.
450

451 **References**

- 452 1. Tong SY, Davis JS, Eichenberger E, Holland TL, Fowler VG, Jr. 2015.
453 *Staphylococcus aureus* infections: epidemiology, pathophysiology, clinical manifestations,
454 and management. *Clin Microbiol Rev* 28:603-61.
- 455 2. Poudel S, Tsunemoto H, Seif Y, Sastry AV, Szubin R, Xu S, Machado H, Olson CA,
456 Anand A, Pogliano J, Nizet V, Palsson BO. 2020. Revealing 29 sets of independently
457 modulated genes in *Staphylococcus aureus*, their regulators, and role in key physiological
458 response. *Proc Natl Acad Sci U S A* 117:17228-17239.
- 459 3. Balasubramanian D, Harper L, Shopsin B, Torres VJ. 2017. *Staphylococcus aureus*
460 pathogenesis in diverse host environments. *Pathog Dis* 75.
- 461 4. Onyango LA, Alreshidi MM. 2018. Adaptive Metabolism in Staphylococci: Survival
462 and Persistence in Environmental and Clinical Settings. *J Pathog* 2018:1092632.
- 463 5. Sutak R, Lesuisse E, Tachezy J, Richardson DR. 2008. Crusade for iron: iron uptake
464 in unicellular eukaryotes and its significance for virulence. *Trends Microbiol* 16:261-8.
- 465 6. Kumar S, Bandyopadhyay U. 2005. Free heme toxicity and its detoxification systems
466 in human. *Toxicol Lett* 157:175-188.
- 467 7. Haley KP, Skaar EP. 2012. A battle for iron: host sequestration and *Staphylococcus*
468 *aureus* acquisition. *Microbes Infect* 14:217-27.
- 469 8. Reniere ML, Torres VJ, Skaar EP. 2007. Intracellular metalloporphyrin metabolism in
470 *Staphylococcus aureus*. *Biometals* 20:333-45.
- 471 9. Skaar EP, Humayun M, Bae T, Debord KL, Schneewind O. 2004. Iron-source
472 preference of *Staphylococcus aureus* infections. *Science* 305:1626-1628.
- 473 10. Saillant V, Lipuma D, Ostin E, Joubert L, Boussac A, Guerin H, Brandelet G, Arnoux
474 P, Lechardeur D. 2021. A Novel *Enterococcus faecalis* Heme Transport Regulator (FhtR)
475 Senses Host Heme To Control Its Intracellular Homeostasis. *mBio* 12.

Membrane heme activates HssS

- 476 11. Bibb LA, Schmitt MP. 2010. The ABC transporter HrtAB confers resistance to hemin
477 toxicity and is regulated in a heme-dependent manner by the ChrAS two-component system
478 in *Corynebacterium diphtheriae*. *J Bacteriol* 192:4606-17.
- 479 12. Lechardeur D, Cesselin B, Liebl U, Vos MH, Fernandez A, Brun C, Gruss A, Gaudu
480 P. 2012. Discovery of an intracellular heme-binding protein, HrtR, that controls heme-efflux
481 by the conserved HrtB HrtA transporter in *Lactococcus lactis*. *J Biol Chem* 287:4752-4758.
- 482 13. Torres VJ, Stauff DL, Pishchany G, Bezbradica JS, Gordy LE, Iturregui J, Anderson
483 KL, Dunman PM, Joyce S, Skaar EP. 2007. A *Staphylococcus aureus* regulatory system that
484 responds to host heme and modulates virulence. *Cell Host Microbe* 1:109-19.
- 485 14. Crow A, Greene NP, Kaplan E, Koronakis V. 2017. Structure and
486 mechanotransmission mechanism of the MacB ABC transporter superfamily. *Proc Natl Acad*
487 *Sci U S A* 114:12572-12577.
- 488 15. Okada U, Yamashita E, Neuberger A, Morimoto M, van Veen HW, Murakami S.
489 2017. Crystal structure of tripartite-type ABC transporter MacB from *Acinetobacter*
490 *baumannii*. *Nat Commun* 8:1336.
- 491 16. Greene NP, Kaplan E, Crow A, Koronakis V. 2018. Antibiotic Resistance Mediated
492 by the MacB ABC Transporter Family: A Structural and Functional Perspective. *Front*
493 *Microbiol* 9:950.
- 494 17. Nakamura H, Hisano T, Rahman MM, Tosha T, Shirouzu M, Shiro Y. 2022. Structural
495 basis for heme detoxification by an ATP-binding cassette-type efflux pump in gram-positive
496 pathogenic bacteria. *Proc Natl Acad Sci U S A* 119:e2123385119.
- 497 18. Stauff DL, Skaar EP. 2009. The heme sensor system of *Staphylococcus aureus*.
498 *Contrib Microbiol* 16:120-135.
- 499 19. Mike LA, Dutter BF, Stauff DL, Moore JL, Vitko NP, Aranmolate O, Kehl-Fie TE,
500 Sullivan S, Reid PR, DuBois JL, Richardson AR, Caprioli RM, Sulikowski GA, Skaar EP.

Membrane heme activates HssS

- 501 2013. Activation of heme biosynthesis by a small molecule that is toxic to fermenting
502 *Staphylococcus aureus*. *Proc Natl Acad Sci U S A* 110:8206-11.
- 503 20. Stauff DL, Skaar EP. 2009. *Bacillus anthracis* HssRS signalling to HrtAB regulates
504 haem resistance during infection. *Mol Microbiol* 72:763-778.
- 505 21. Jacob-Dubuisson F, Mechaly A, Betton JM, Antoine R. 2018. Structural insights into
506 the signalling mechanisms of two-component systems. *Nat Rev Microbiol* 16:585-593.
- 507 22. Liu Y, Rose J, Huang S, Hu Y, Wu Q, Wang D, Li C, Liu M, Zhou P, Jiang L. 2017.
508 A pH-gated conformational switch regulates the phosphatase activity of bifunctional HisKA-
509 family histidine kinases. *Nat Commun* 8:2104.
- 510 23. Mideros-Mora C, Miguel-Romero L, Felipe-Ruiz A, Casino P, Marina A. 2020.
511 Revisiting the pH-gated conformational switch on the activities of HisKA-family histidine
512 kinases. *Nat Commun* 11:769.
- 513 24. Joubert L, Dagieu JB, Fernandez A, Derre-Bobillot A, Borezee-Durant E, Fleurot I,
514 Gruss A, Lechardeur D. 2017. Visualization of the role of host heme on the virulence of the
515 heme auxotroph *Streptococcus agalactiae*. *Sci Rep* 7:40435.
- 516 25. Joubert L, Derre-Bobillot A, Gaudu P, Gruss A, Lechardeur D. 2014. HrtBA and
517 menaquinones control haem homeostasis in *Lactococcus lactis*. *Mol Microbiol* 93:823-33.
- 518 26. Shah N, Gaupp R, Moriyama H, Eskridge KM, Moriyama EN, Somerville GA. 2013.
519 Reductive evolution and the loss of PDC/PAS domains from the genus *Staphylococcus*. *BMC*
520 *Genomics* 14:524.
- 521 27. Anzaldi LL, Skaar EP. 2010. Overcoming the heme paradox: heme toxicity and
522 tolerance in bacterial pathogens. *Infect Immun* 78:4977-4989.
- 523 28. Fritz G, Dintner S, Treichel NS, Radeck J, Gerland U, Mascher T, Gebhard S. 2015. A
524 New Way of Sensing: Need-Based Activation of Antibiotic Resistance by a Flux-Sensing
525 Mechanism. *MBio* 6:e00975.

Membrane heme activates HssS

- 526 29. Mascher T. 2014. Bacterial (intramembrane-sensing) histidine kinases: signal transfer
527 rather than stimulus perception. *Trends Microbiol* 22:559-65.
- 528 30. Mascher T, Helmann JD, Uden G. 2006. Stimulus perception in bacterial signal-
529 transducing histidine kinases. *Microbiol Mol Biol Rev* 70:910-38.
- 530 31. Gebhard S. 2012. ABC transporters of antimicrobial peptides in Firmicutes bacteria -
531 phylogeny, function and regulation. *Mol Microbiol* 86:1295-317.
- 532 32. Gebhard S, Mascher T. 2011. Antimicrobial peptide sensing and detoxification
533 modules: unravelling the regulatory circuitry of *Staphylococcus aureus*. *Mol Microbiol*
534 81:581-7.
- 535 33. Dintner S, Staron A, Berchtold E, Petri T, Mascher T, Gebhard S. 2011. Coevolution
536 of ABC transporters and two-component regulatory systems as resistance modules against
537 antimicrobial peptides in Firmicutes Bacteria. *J Bacteriol* 193:3851-62.
- 538 34. Kenanian G, Morvan C, Weckel A, Pathania A, Anba-Mondoloni J, Halpern D,
539 Gaillard M, Solgadi A, Dupont L, Henry C, Poyart C, Fouet A, Lamberet G, Gloux K, Gruss
540 A. 2019. Permissive Fatty Acid Incorporation Promotes Staphylococcal Adaptation to FASII
541 Antibiotics in Host Environments. *Cell Rep* 29:3974-3982 e4.
- 542 35. Orelle C, Mathieu K, Jault JM. 2019. Multidrug ABC transporters in bacteria. *Res*
543 *Microbiol* 170:381-391.
- 544 36. Skaar EP, Schneewind O. 2004. Iron-regulated surface determinants (Isd) of
545 *Staphylococcus aureus*: stealing iron from heme. *Microbes Infect* 6:390-7.
- 546 37. Caldelari I, Chane-Woon-Ming B, Noirot C, Moreau K, Romby P, Gaspin C, Marzi S.
547 2017. Complete Genome Sequence and Annotation of the *Staphylococcus aureus* Strain
548 HG001. *Genome Announc* 5.
- 549 38. Ghssein G, Brutesco C, Ouerdane L, Fojcik C, Izaute A, Wang S, Hajjar C, Lobinski
550 R, Lemaire D, Richaud P, Voulhoux R, Espaillat A, Cava F, Pignol D, Borezee-Durant E,

Membrane heme activates HssS

- 551 Arnoux P. 2016. Biosynthesis of a broad-spectrum nicotianamine-like metallophore in
552 *Staphylococcus aureus*. *Science* 352:1105-9.
- 553 39. Taylor D, Holland KT. 1989. Amino acid requirements for the growth and production
554 of some exocellular products of *Staphylococcus aureus*. *J Appl Bacteriol* 66:319-29.
- 555 40. Ebner P, Rinker J, Nguyen MT, Popella P, Nega M, Luqman A, Schittek B, Di Marco
556 M, Stevanovic S, Gotz F. 2016. Excreted Cytoplasmic Proteins Contribute to Pathogenicity in
557 *Staphylococcus aureus*. *Infect Immun* 84:1672-81.
- 558 41. Berry EA, Trumpower BL. 1987. Simultaneous determination of hemes a, b, and c
559 from pyridine hemochrome spectra. *Anal Biochem* 161:1-15.
- 560 42. Humphrey W, Dalke A, Schulten K. 1996. VMD: visual molecular dynamics. *J Mol*
561 *Graph* 14:33-8, 27-8.
- 562 43. Poyart C, Trieu-Cuot P. 1997. A broad-host-range mobilizable shuttle vector for the
563 construction of transcriptional fusions to B-galactosidase in Gram-positive bacteria. *FEMS*
564 *Microbiology Letters* 156:193-198.
- 565 44. Arnaud M, Chastanet A, Debarbouille M. 2004. New vector for efficient allelic
566 replacement in naturally nontransformable, low-GC-content, gram-positive bacteria. *Appl*
567 *Environ Microbiol* 70:6887-91.
- 568 45. Kreiswirth BN, Lofdahl S, Betley MJ, O'Reilly M, Schlievert PM, Bergdoll MS,
569 Novick RP. 1983. The toxic shock syndrome exotoxin structural gene is not detectably
570 transmitted by a prophage. *Nature* 305:709-12.
- 571 46. Charpentier E, Anton AI, Barry P, Alfonso B, Fang Y, Novick RP. 2004. Novel
572 cassette-based shuttle vector system for gram-positive bacteria. *Appl Environ Microbiol*
573 70:6076-85.
- 574 47. Wada A, Watanabe H. 1998. Penicillin-binding protein 1 of *Staphylococcus aureus* is
575 essential for growth. *J Bacteriol* 180:2759-65.

Membrane heme activates HssS

576 48. Toledo-Arana A, Merino N, Vergara-Irigaray M, Debarbouille M, Penades JR, Lasa I.
577 2005. Staphylococcus aureus develops an alternative, ica-independent biofilm in the absence
578 of the arlRS two-component system. J Bacteriol 187:5318-29.

579

580 **Figure legends**

581 **Figure 1.** P_{hrtBA} induction reports HssS activity. (A) HssS and HrtB expressions in presence of
582 heme. *S. aureus* HG001 $\Delta hssRS$ (p_{hssRS} -HA) was incubated with the indicated concentrations
583 of hemin. WB on bacterial lysates was performed with anti-HA and anti-HrtB antibodies.
584 Result is representative of 3 independent experiments. (B, C) *hssRS* and *hrtBA* transcription
585 regulation by exogenous heme. *S. aureus* HG001 transformed with p_{hssRS} -*lac* (B) or p_{hrtBA} -
586 *lac* (C) were grown in BHI to $OD_{600} = 0.5$ prior addition of the indicated concentration of
587 hemin for 1.5 h. β -gal activity was quantified by luminescence. Results represent the average
588 \pm S.D. from triplicate independent experiments. ****, $P < 0.0001$; ns, non-significant,
589 Student's *t* test. (D) P_{hrtBA} is not induced in the HG001 $\Delta hssRS$ mutant. WT and $\Delta hssRS$
590 HG001 strains transformed with p_{hrtBA} -*lac* were grown and β -gal activity determined as in
591 (B-C) with 1 μ M hemin. Results represent the average \pm S.D. from triplicate independent
592 experiments. ***, $P < 0.001$, Student's *t* test.

593 **Figure 2.** HssS transient activation reports intracellular accumulation of exogenous heme. (A)
594 Dynamics of P_{hrtBA} induction in *S. aureus* HG001 by exogenous heme. Bacteria transformed
595 with p_{hrtBA} -GFP were diluted from an ON culture to $OD_{600} = 0.01$ in CDM with the indicated
596 concentration of hemin in a microplate spectrofluorimeter Infinite (Tecan). Both fluorescence
597 (Exc: 475 nm; Em: 520 nm) and OD_{600} were recorded every 5 min for the indicated time.
598 Fluorescence (RFU) at each time point was divided by the corresponding OD_{600} . Results of
599 hemin induced fluorescence minus non-induced (background, 0 μ M hemin) are displayed.
600 Results represent the average \pm S.D. from triplicate biological samples. The corresponding
601 growth curves are shown. (B) Phosphatase activity of HssS. $\Delta hssRS$ HG001 transformed with
602 p_{GFP} (HssS) or p_{GFP} (HssS T253A) were diluted in CDM \pm 1 μ M hemin from an ON culture
603 in 96-microplate as in (A). Fluorescence emission was quantified as in (A). Fluorescence
604 (RFU) at each time point was divided by the corresponding OD_{600} . Results of hemin induced

Membrane heme activates HssS

605 fluorescence minus non-induced (background, 0 μ M hemin) are displayed. Results represent
606 the average \pm S.D. from triplicate biological samples. ****, $P < 0.0001$, Student's t test. The
607 corresponding growth curves are shown. (C) Dynamics of P_{hrtBA} induction in WT and $\Delta hrtBA$
608 HG001 strains by exogenous heme. *S. aureus* HG001 WT and $\Delta hrtBA$ strains transformed
609 with pP_{hrtBA} -GFP were diluted from an ON culture to $OD_{600} = 0.01$ in CDM with 1 μ M hemin
610 in a 96 well microplate. OD_{600} and GFP expression were followed in a spectrofluorimeter
611 Infinite (Tecan) as in Fig. 1. Results of hemin induced fluorescence minus non-induced
612 (background, 0 μ M hemin) are displayed Results represent the average \pm S.D. from triplicate
613 biological samples. The corresponding growth curve are shown. ****, $P < 0.0001$, Student's t
614 test. (D) Dynamics of HssS activation in HG001 WT and $\Delta hrtBA$ strains by hemoglobin.
615 Fluorescence emission kinetic was followed as in (C) in HG001 WT and $\Delta hrtBA$ strains
616 transformed pP_{hrtBA} -GFP with 0.25 μ M human hemoglobin (equivalent to 1 μ M hemin) added
617 to the culture medium. Results represent the average \pm S.D. from triplicate technical samples
618 and are representative of 3 independent experiments. ****, $P < 0.0001$, Student's t test. The
619 corresponding growth curves are shown.

620 **Figure 3.** Alphafold structural model the HssS and heme docking solutions. (A) Alphafold
621 model of *Staphylococcus aureus* HssS dimer, with one chain colored in green and the other in
622 grey. The position of the membrane proposed by the OPM server is shown by red and blue
623 spheres. (B) Superimposition of all the docking solutions using the ECD domains of HssS.
624 These solutions are all < -8 kcal/mol and suggest the presence of two docking sites, which
625 represents a single binding site due to the two-fold symmetry of the dimer. This binding site is
626 located at the interface between the membrane and the extracellular space. (C) Electrostatic
627 surface potential calculated with APBS with a ramp from -5 kTe (red) to +5 kTe (blue). (D)
628 Mapping of sequence conservation on the surface of the model depicts only a few solvent
629 exposed conserved residues. (E) Superimposition of the best docking solution of heme

Membrane heme activates HssS

630 (colored in grey) with with predicted residues within 5Å. Cartoon and residues are colored
631 according to sequence conservation (Fig. 3A) and only conserved residues are shown in stick.

632 **Figure 4.** Pivotal roles of Arg94 and Arg163 on HssS activation. (A) P_{hrtBA} transcriptional
633 induction by HssS, HssS R94A and HssS R163A. Kinetics of P_{hrtBA} induction in
634 HG001 $\Delta hssRS$ mutant transformed either with pGFP(HssS), pGFP(HssS R94A) or
635 pGFP(HssS R163A). Strains from ON cultures were diluted to $OD_{600} = 0.01$ in CDM $\pm 1 \mu\text{M}$
636 of hemin in a 96 well microplate. OD_{600} and GFP expression were followed in a
637 spectrofluorimeter Infinite (Tecan) as in Fig. 2. Results of hemin induced fluorescence minus
638 non-induced (background, 0 μM hemin) are displayed. Results represent the average \pm S.D.
639 from triplicate biological samples. ****, $P < 0.0001$, Student's t test. The corresponding
640 growth curves are shown. (B) Comparative expressions of HssS-HA, HssS-HA R94A, HssS-
641 HA R163A and HrtB. Strains as in (A) were diluted in BHI from ON culture at $OD_{600} = 0.01$.
642 Cultures were supplemented $\pm 1 \mu\text{M}$ hemin and grown for 1.5 h. HG001 $\Delta hssRS$ transformed
643 with the empty plasmid (\emptyset) was used as a control. HssS-HA and HrtB expression were
644 monitored on bacterial lysates by Western Blot (WB) with an anti-hemagglutinin antibody (α -
645 HA) and an anti-HrtB antibody respectively (α -HrtB). Results are representative of three
646 independent experiments. (C) Hemin toxicity in HssS, HssS R94A and HssS R163A
647 expressing strains. Strains as in (B) were diluted from an ON preculture to an OD_{600} of 0.01 in
648 BHI supplemented with 20 μM hemin and grown in a 96 microplate. (Growth curves were
649 similar for all strains grown without hemin (Fig. S5A)). OD_{600} was recorded every 20 min for
650 the indicated time in a spectrophotometer (Spark, Tecan). Results represent the average \pm S.D
651 from triplicate biological samples.

652 **Figure 5.** Impact of the heme binding hydrophobic environment on HssS activation. (A) P_{hrtBA}
653 transcriptional induction by HssS, HssS F25A, HssS F128A and HssS F165A. Kinetics of

Membrane heme activates HssS

654 P_{hrtBA} induction in HG001 $\Delta hssRS$ mutant transformed either with pGFP(HssS), pGFP(HssS
655 R25A), pGFP(HssS F128A) or pGFP(HssS F165A) was performed as in Fig. 4. Results of
656 hemin induced fluorescence minus non-induced (background, 0 μ M hemin) are displayed.
657 Results represent the average \pm S.D. from triplicate biological samples. ****, $P < 0.0001$,
658 Student's t test. The corresponding growth curves are shown. (B) Comparative expressions of
659 HssS-HA, HssS-HA F25A, HssS-HA F128A, HssS-HA F165A and HrtB. Strains as in (A)
660 were diluted in BHI from ON culture at $OD_{600} = 0.01$. Cultures were supplemented $\pm 1 \mu$ M
661 hemin and grown for 1.5 h. HG001 $\Delta hssRS$ transformed with the empty plasmid (\emptyset) was used
662 as a control. HssS-HA and HrtB expression were monitored on bacterial lysates by Western
663 Blot (WB) as in Fig. 4. Results are representative of three independent experiments. (C)
664 Hemin toxicity in HssS, HssS F25A, HssS F128A and HssS F165A expressing strains. Strains
665 as in (B) were diluted from an ON preculture to an OD_{600} of 0.01 in BHI supplemented with
666 20 μ M hemin and grown in a 96 microplate as in Fig. 4. (Growth curves were similar for all
667 strains grown without hemin (Fig. S5B). Results represent the average \pm S.D from triplicate
668 biological samples. (D) Pymol representation of the relative positions of F25, F128 and F165
669 to hemin in the predicted heme binding domain of HssS.

670 **Figure 6.** Inhibition of the heme sensing activity of HssS R94A, R163A, F25A, F128A (4
671 mut.). (A) HssS-4 mut. is unable to induce P_{hrtBA} transcription. Kinetics of P_{hrtBA} induction in
672 HG001 $\Delta hssRS$ mutant transformed either with pGFP(HssS) or pGFP(HssS 4 mut.) was
673 performed as in Fig. 4. Results of hemin induced fluorescence minus non-induced
674 (background, 0 μ M hemin) are displayed. Results represent the average \pm S.D. from triplicate
675 biological samples. ****, $P < 0.0001$, Student's t test. The corresponding growth curves are
676 shown. (B) Comparative expressions of HssS-HA, HssS-HA 4 mut. and HrtB. Strains as in
677 (A) were diluted in BHI from ON culture at $OD_{600} = 0.01$. Cultures were supplemented ± 1
678 μ M hemin and grown for 1.5 h. HG001 $\Delta hssRS$ transformed with the empty plasmid (\emptyset) was

Membrane heme activates HssS

679 used as a control. HssS-HA and HrtB expression were monitored on bacterial lysates by
680 Western Blot (WB) as in Fig. 4. Results are representative of three independent experiments.
681 (C) Hemin toxicity in HssS and HssS 4 mut. expressing strains. Strains as in (B) were diluted
682 from an ON preculture to an OD₆₀₀ of 0.01 in BHI supplemented with 20 μM hemin and
683 grown in a 96 microplate as in Fig. 4. (Growth curves were similar for all strains grown
684 without hemin (Fig. S5C). Results represent the average ± S.D from triplicate biological
685 samples.

686 **Figure 7.** The extracellular domain is required for heme dependent activation of HssS. (A-B)
687 Comparative dynamics of P_{hrtBA} transcriptional induction by HssS WT and HssS ΔECD
688 HG001 in absence (A) or in presence of hemin (B). HG001 Δ*hssRS* mutant transformed with
689 either pGFP(HssS), pGFP(HssS ΔECD) or empty vector were grown as in Fig. 2 in CDM
690 without heme (A) or supplemented with 1 μM of hemin (B). Fluorescence (RFU) and OD₆₀₀
691 were determined as in Fig. 2. Results of fluorescence (RFU/OD₆₀₀) from strains expressing
692 HssS WT or HssS ΔECD minus empty vector transformed strain are displayed. Results
693 represent the average ± S.D. from triplicate biological samples. The corresponding growth
694 curves are shown. (C) HssS ΔECD constitutively signals HrtB expression. Δ*hssRS* HG001
695 transformed either with pGFP(HssS), pGFP(HssS ΔECD) or empty vector (∅) were used to
696 monitor HssS and HrtB expression by WB with α-HA and an α-HrtB, respectively. Bacteria
697 were grown to an OD₆₀₀=0.5 and induced for 1.5 h ± 1 μM hemin. SDS-PAGE was performed
698 on cell lysates (25 μg per lane). Results are representative of three independent experiments.

699 **Figure 8.** Functional model of exogenous heme management by the gatekeeping HssRS-
700 HrtBA system in *S. aureus*. Exogenous hemin (red dots) translocates through the membrane
701 (Mb) compartment from the extracellular (EC) to the intracellular (IC) compartments. HssS
702 senses heme at the membrane interface, activating the phosphorelay between the HK and

Membrane heme activates HssS

703 HssR leading to the expression of HrtBA. The pool of heme that crosses the membrane by
704 diffusion is counterbalanced by HrtBA which extrudes heme from the membrane to EC space
705 (17).

706

707

708

709

710 Supplemental Information

711 **Plasmid construction.** Plasmid pTCV-*lac* is a low copy number plasmid that uses the
712 *lac* gene as a reporter to evaluate promoter activities in Gram-positive bacteria (43) (*SI*
713 *Appendix*, Table S1). DNA fragments containing the *hrtBA* or the *hssRS* promoter were PCR-
714 amplified with primer pairs (O1-O2) or (O3-O4) (*SI Appendix*, Table S2) respectively. The
715 amplified fragments were digested with *EcoRI/BamHI* and cloned into pTCV-*lac*, resulting in
716 plasmids pP_{hrtBA}-*lac* and pP_{hssRS}-*lac* (*SI Appendix*, Table S1). pP_{hrtBA}-GFP (*SI Appendix*, Table
717 S2) was constructed by cloning fragments corresponding to P_{hrtBA} with the primer pairs (O5-
718 O6) and into the *BamHI/EcoRI* restriction sites of the pCN52 vector (*SI Appendix*, Table S1)
719 using HG001 genomic DNA as template. The DNA sequence of P_{hssRS} *hssRS*-HA was PCR
720 amplified from the plasmid pUC *hssRS*-HA-P_{hrtBA} with oligonucleotides (O7-O8) (*SI*
721 *Appendix*, Table S2), digested with *BamHI/KpnI* and ligated into pCN52 to give rise to
722 p*hssRS*-HA, P_{hrtBA}-GFP (pGFP(HssS)) (*SI Appendix*, Table S1). *hssS* gene is followed by the
723 nt sequence encoding the hemagglutinin influenza epitope (HA, YPYDVPDYA). p*hssRS*-HA
724 ΔECL, P_{hrtBA}-GFP (pGFP (HssS ΔECL)) was obtained by an overlap of two PCRs amplified
725 with the primer pairs (O7-O9) and (O8-O10) (*SI Appendix*, Table S2) using pUC *hssRS*-HA-
726 P_{hrtBA} as a template. The P_{hssRS}*hssRS*-HA ΔECL fragment digested with *BamHI/KpnI* and
727 ligated into pCN52 to give rise to pGFP (HssS ΔECL) (*SI Appendix*, Table S1). The DNA
728 sequence corresponding to extracellular domain of HrtB was PCR amplified with primers pair
729 (O11-O12) using HG001 genomic DNA as a template that was cloned into the *E. coli*
730 expression vector pET200 as recommended by the manufacturer's instructions to generate
731 pET200-*hrtB* ECL (*SI Appendix*, Table S1). The pMADΔ*hrtBA* plasmid was constructed as
732 follows: 2 DNA fragments of ~800 bp flanking the *hrtBA* operon were PCR-amplified using
733 *S. aureus* HG001 genomic DNA as a template and primer pairs (O13-O14) and (O15-O16) (*SI*
734 *Appendix*, Table S2). Both fragments were used as templates in a second round of PCR

Membrane heme activates HssS

735 amplification with primers (O13-O16), resulting in an overlapping ~1.6 kb fragment, which
736 was digested by *Xma*I and *Bam*HI and cloned into the thermosensitive plasmid, pMAD (2),
737 giving rise to p Δ *hrtBA* (*SI Appendix*, Table S1). p Δ *hrtBA* was established by transformation in
738 *S. aureus* HG001. The double cross-over event leading to the Δ *hrtBA* mutant was obtained as
739 described (44). *phssRS*-HA was constructed by PCR amplification of the *hssRS*-HA sequence
740 from the pUC *hssRS*-HA-*P_{hrtBA}* plasmid with (O16-O17). The amplified *P_{hssRS}* *hssRS*-HA
741 DNA fragment was cloned into *Pst*I/*Bam*HI restriction sites of PAW8 (*SI Appendix*, Table
742 S1). All plasmids were verified by DNA sequencing.

743

744 1. Poyart C, Trieu-Cuot P. 1997. A broad-host-range mobilizable shuttle vector for the
745 construction of transcriptional fusions to B-galactosidase in Gram-positive bacteria. *FEMS*
746 *Microbiology Letters* 156:193-198.

747 2. Arnaud M, Chastanet A, Debarbouille M. 2004. New vector for efficient allelic
748 replacement in naturally nontransformable, low-GC-content, gram-positive bacteria. *Appl*
749 *Environ Microbiol* 70:6887-91.

750

751

752

753

754

755 **Supplemental Tables**

756 **Table S1.** Strains and plasmids used in this study.

<i>Strain/plasmid</i>	<i>Characteristics</i>	<i>Source/reference</i>
Strain		
<i>E. coli</i>		
TOP10	<i>F⁻ mcrA Δ(mrr-hsdRMS-mcrBC) Δ80lacZΔM15 lacX74 recA1 deoR araD139 Δ(ara-leu)7697 galU galK rpsL (Str^r) endA1</i>	Invitrogen
BL21 (DE3)	<i>lacI^q rrnB T14 ΔlacZΔWJ16 hsdR514 ΔaraBA-D_{AH33} ΔrhaBAD_{LD78}</i>	Invitrogen
<i>S. aureus</i>		
RN4220	<i>S. aureus</i> cloning recipient ATCC 8325-4 derivative restriction negative	(45)
HG001	<i>Staphylococcus aureus</i> HG001 strain, derivative of the RN1 (NCT8325) strain with restored rbsU (a positive activator of SigB).	(37)
HG001H1	HG001 Δ <i>hssRS</i> , deletion of <i>hssR</i> and <i>hssS</i> genes	This study
HG001H2	HG001 Δ <i>hrtBA</i> , deletion of <i>hrtB</i> and <i>hrtA</i> genes	This study
Plasmid		
pTCV- <i>lac</i>	Conjugative <i>E. coli</i> Gram-positive bacteria shuttle plasmid carrying the promoter less <i>E. coli lacZ</i> gene for constructing transcriptional fusions. Kan ^R , Ery ^R	(43)
pCN52	<i>E. coli-S.aureus</i> bacteria shuttle plasmid with <i>gfpmut2</i> reporter construct. Amp ^R , Ery ^R	(46)
pAW8	Cloning shuttle vector, pMB1 ori for replication in <i>E. coli</i> , pAMα1 ori for replication in gram-positive organisms. Tet ^R , Amp ^R	(47)
pMAD	Cloning shuttle replication-thermosensitive vector for generating stable chromosomal mutations in low G-C Gram positive bacteria. Amp ^R , Ery ^R	(44)
pP _{<i>hrtBA</i>} - <i>lac</i>	<i>S. aureus</i> HG001 <i>hrtBA</i> promoter region cloned into pTCV- <i>lac</i> . Kan ^R , Ery ^R	This study

Membrane heme activates HssS

pP _{hssRS-lac}	<i>S. aureus</i> HG001 <i>hssRS</i> promoter region region cloned into pTCV- <i>lac</i> . Kan ^R , Ery ^R	This study
pUC <i>hssRS</i> -HA, P _{hrtBA}	P _{hssRS} promoter region and <i>hssRS</i> genes followed by the promoter region of <i>hrtBA</i> from <i>S. aureus</i> HG001 cloned into pUC. Amp ^R	Proteogenix (France)
p <i>hssRS</i> -HA	<i>hssRS</i> promoter region and <i>hssRS</i> genes with a HA epitope at the Ct of <i>hssS</i> from <i>S. aureus</i> HG001 in pAW8. Tet ^R , Amp ^R	This study
pP _{hrtBA-gfp}	<i>S. aureus</i> HG001 <i>hrtBA</i> promoter region cloned into pCN52. Amp ^R , Ery ^R	This study
pGFP(HssS)	p <i>hssRS</i> -HA, P _{hrtBA-gfp} . Promoter region and <i>hssRS</i> genes with a HA epitope at the Ct of <i>hssS</i> from <i>S. aureus</i> HG001 and promoter region of <i>hrtBA</i> cloned upstream GFP in pCN52. Amp ^R , Ery ^R	This study
pGFP(HssS T253A)	p <i>hssRS</i> -HA T253A, P _{hrtBA-gfp} . pGFP(HssS) plasmid with a mutation of the codon encoding T253 to alanine codon in <i>hssS</i> . Amp ^R , Ery ^R	E-Zyvec (France)
pGFP(HssS R94A)	p <i>hssRS</i> -HA R94A, P _{hrtBA-gfp} . pGFP(HssS) plasmid with a mutation of the codon encoding R94 to alanine codon in <i>hssS</i> . Amp ^R , Ery ^R	E-Zyvec (France)
pGFP(HssS R163A)	p <i>hssRS</i> -HA R163A, P _{hrtBA-gfp} . pGFP(HssS) plasmid with a mutation of the codon encoding R163 to alanine codon in <i>hssS</i> . Amp ^R , Ery ^R	E-Zyvec (France)
pGFP(HssS R94A, R163A)	p <i>hssRS</i> -HA R94A, R163A, P _{hrtBA-gfp} . pGFP(HssS) plasmid with mutations of the codon encoding R94 and R163 to alanine codon in <i>hssS</i> . Amp ^R , Ery ^R	E-Zyvec (France)
pGFP(HssS F25A)	p <i>hssRS</i> -HA F25A, P _{hrtBA-gfp} . pGFP(HssS) plasmid with a mutation of the codon encoding F25 to alanine codon in <i>hssS</i> . Amp ^R , Ery ^R	E-Zyvec (France)
pGFP(HssS F128A)	p <i>hssRS</i> -HA F128A, P _{hrtBA-gfp} . pGFP(HssS) plasmid with a mutation of the codon encoding F128 to alanine codon in <i>hssS</i> . Amp ^R , Ery ^R	E-Zyvec (France)
pGFP(HssS F165A)	p <i>hssRS</i> -HA F165A, P _{hrtBA-gfp} . pGFP(HssS) plasmid with a mutation of the codon encoding F165 to alanine codon in <i>hssS</i> . Amp ^R , Ery ^R	E-Zyvec (France)
pGFP(HssS4 mut.)	p <i>hssRS</i> -HA R94A, R163A, F128A, F165A, P _{hrtBA-gfp} . pGFP(HssS) plasmid with mutations of the codon encoding R94, R163, F25, F128 to alanine codon in <i>hssS</i> . Amp ^R , Ery ^R	E-Zyvec (France)
pGFP(HssS ΔECL)	p <i>hssRS</i> ΔECL-HA, P _{hrtBA-gfp} . pGFP(HssS) plasmid with a deletion of the nucleotides corresponding to the AA [50-129] of HssS. Amp ^R , Ery ^R	This study
pΔ <i>hssRS</i>	<i>hssRS</i> fragment cloned into pMAD to obtain the HG001-Δ <i>hssRS</i> mutant.	(48)
pΔ <i>hrtBA</i>	<i>hrtBA</i> fragment cloned into pMAD to obtain the HG001 Δ <i>hrtBA</i> mutant. Amp ^R , Ery ^R	This study

Membrane heme activates HssS

- 757 1. Kreiswirth BN, Lofdahl S, Betley MJ, O'Reilly M, Schlievert PM, Bergdoll MS,
758 Novick RP. 1983. The toxic shock syndrome exotoxin structural gene is not detectably
759 transmitted by a prophage. *Nature* 305:709-12.
- 760 2. Caldelari I, Chane-Woon-Ming B, Noirot C, Moreau K, Romby P, Gaspin C, Marzi S.
761 2017. Complete Genome Sequence and Annotation of the *Staphylococcus aureus* Strain
762 HG001. *Genome Announc* 5.
- 763 3. Poyart C, Trieu-Cuot P. 1997. A broad-host-range mobilizable shuttle vector for the
764 construction of transcriptional fusions to B-galactosidase in Gram-positive bacteria. *FEMS*
765 *Microbiology Letters* 156:193-198.
- 766 4. Charpentier E, Anton AI, Barry P, Alfonso B, Fang Y, Novick RP. 2004. Novel
767 cassette-based shuttle vector system for gram-positive bacteria. *Appl Environ Microbiol*
768 70:6076-85.
- 769 5. Wada A, Watanabe H. 1998. Penicillin-binding protein 1 of *Staphylococcus aureus* is
770 essential for growth. *J Bacteriol* 180:2759-65.
- 771 6. Arnaud M, Chastanet A, Debarbouille M. 2004. New vector for efficient allelic
772 replacement in naturally nontransformable, low-GC-content, gram-positive bacteria. *Appl*
773 *Environ Microbiol* 70:6887-91.
- 774 7. Toledo-Arana A, Merino N, Vergara-Irigaray M, Debarbouille M, Penades JR, Lasa I.
775 2005. *Staphylococcus aureus* develops an alternative, ica-independent biofilm in the absence
776 of the arlRS two-component system. *J Bacteriol* 187:5318-29.

777

778

779 **Table S2.** Oligonucleotides used in this study.

<i>Primer</i>	<i>Sequence 5'-3'</i>	<i>Target</i>
O1	ATTTTAGAATTCGCACCATAGCTATAAACT	pP _{hrtBA} -lac
O1	ATTTTAGGATCCATCGATTCACTTCTCCCT	pP _{hrtBA} -lac
O3	ATTTTAGAATTCGATCCATCGATTCACTTC	pP _{hssRS} -lac
O4	TAAAATGGATCCAGCTATAAACTCCCTTAT	pP _{hssRS} -lac
O5	TTACCGGAATTCATCGATTCACTTCTCCCT	pP _{hrtBA} -gfp
O6	AATCGCGGATCCAGCTATAAACTCCCTTAT	pP _{hrtBA} -gfp
O7	ATAATAGGATCCTTAAGCATAATCTGGAAC	pGFP(HssS)
O8	TAATAAGGTACCATCGATTCACTTCTCCCT	pGFP(HssS)
O9	AATATCTGGACGCATATTAGATGCTTTTAA	pGFP(HssS ΔECL)
O10	TTAAAAGCATCTAATATGCGTCCAGATATT	pGFP(HssS ΔECL)
O11	CACCTCGTTATTTGAACACTTTGATA	pET200-hrtB ECL
O12	TTAACTAACAATCATCATATTT	pET200-hrtB ECL
O13	TTAATTGGATCCACTGTTTCAATTG	pMAD ΔhrtBA
O14	CGTCTTTACAAGCCAATCGATTCACTTCTC	pMAD ΔhrtBA
O15	GAGAAGTGAATCGATTGGCTTGTAAGACG	pMAD ΔhrtBA
O16	AATTAACCCGGGGTGCCGTCTCAGC	pMAD ΔhrtBA
O17	GGGGCTGCAGCTCCCTATTTCTTCTTTAGCG	phssRS-HA
O28	AATTAAGGATCCTTAAGCATAATCTGGAACATCATAT GGATACAT	phssRS-HA

780

781

782

783

784

785

786 **Supplemental figures**

787 **Figure S1.** Transient induction of P_{hrtBA} during stationary and exponential growth phases. (A)
788 Kinetic of P_{hrtBA} induction in stationary phase. HG001 WT and $\Delta hrtBA$ strains transformed
789 with pP_{hrtBA} -GFP. ON culture in CDM were distributed in a 96 well microplate. OD_{600} and
790 GFP expression were followed in a spectrofluorimeter Infinite (Tecan). Results of hemin
791 induced fluorescence minus non-induced (background, 0 μ M hemin) are displayed. Results
792 represent the average \pm S.D. from triplicate biological samples. (B) Kinetic of HrtB
793 expression following addition of hemin in HG001 WT. Strain from ON culture was diluted to
794 $OD_{600} = 0.1$ in BHI. 2 μ M hemin were added to the culture at $t=0$. At the indicated time
795 points, samples of bacteria (containing equivalent number of bacteria) were pelleted and OD
796 normalized to 0.5 by resuspending the pellet in PBS. At the indicated time point, samples of
797 bacteria were pelleted and processed for SDS-PAGE and immunoblot with a α -HrtB
798 antibody.

799 **Figure S2.** Heme accumulates in HG001 $\Delta hrtBA$ strain. WT and $\Delta hrtBA$ strains were grown
800 to $OD_{600} = 1$ prior addition of 10 μ M hemin in BHI for an additional 1.5 h. (A) Bacteria
801 were pelleted by centrifugation and photographed. (B) Heme content in the cell pellets was
802 determined by the pyridine hemochrome assay on lysates. Background from bacteria non-
803 exposed to hemin was subtracted. Results represent the average \pm S.D. from biological
804 triplicates. *, $P=0.045$, Student's t test.

805 **Figure S3.** Superimposition of all the docking solutions using the intracellular part of HssS.
806 As compared to Fig 3B using the ECD of HssS, all the docking solutions are above -8
807 kcal/mol and are scattered on the surface of the protein.

Membrane heme activates HssS

808 **Figure S4.** WebLogo representation of AAs [1-188] of HssS. Residues targeted by site-
809 directed mutagenesis are highlighted by a red asterisk (orange for phenylalanine, pink for
810 arginines). Red line represents the ECD.

811 **Figure S5.** Growth of HG001 $\Delta hssRS$ complemented either with pGFP(HssS) or HssS
812 variants R94A, R163A, F25A, F128A, F165A. All strains were diluted from an ON
813 preculture to an OD₆₀₀ of 0.01 in CDM and grown in a microplate. OD₆₀₀ was recorded every
814 20 min for the indicated time in a spectrophotometer (Spark, Tecan). (A) Growth of $\Delta hssRS$
815 mutants transformed either with pGFP(HssS), pGFP(HssS R94A), pGFP(HssS R163A),
816 pGFP(HssS R94A, R163A) or empty vector (p \emptyset). Results represent the average \pm S.D from
817 triplicate biological samples. (B) Growth of $\Delta hssRS$ mutants transformed either with
818 pGFP(HssS), pGFP(HssS F25A), pGFP(HssS F128A), pGFP(HssS F165A) or empty vector
819 (p \emptyset). Results of bacterial growth minus medium background are displayed. Results represent
820 the average \pm S.D from triplicate biological samples. (C) Growth of $\Delta hssRS$ mutants
821 transformed either with pGFP(HssS), pGFP(HssS 4 mut.) or empty vector (p \emptyset). Results of
822 bacterial growth minus medium background are displayed. Results represent the average \pm
823 S.D from triplicate biological samples.

824 **Figure S6.** HssS Δ ECD is expressed at the membrane and signals heme detoxification. (A)
825 Cell fractionation of HssS FL and Δ ECD expressing HG001 bacteria. $\Delta hssRS$ HG001
826 transformed with either pGFP(HssS) or pGFP(HssS Δ ECD) were grown in BHI to an OD₆₀₀ =
827 1, lysed and processed for the separation of membrane from cytoplasm by ultracentrifugation.
828 Whole cell lysate, isolated membrane and cytoplasm enriched fractions were processed for
829 SDS-PAGE and immunoblot using an anti-HA antibody. An anti-GAPDH antibody was used
830 as a marker of cytoplasm. Result is representative of 3 independent experiments. (B-C) Heme
831 toxicity in liquid culture of $\Delta hssRS$ HG001 transformed with either pGFP(HssS),

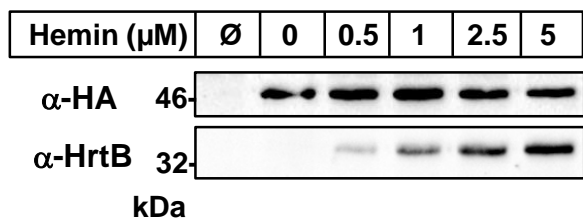
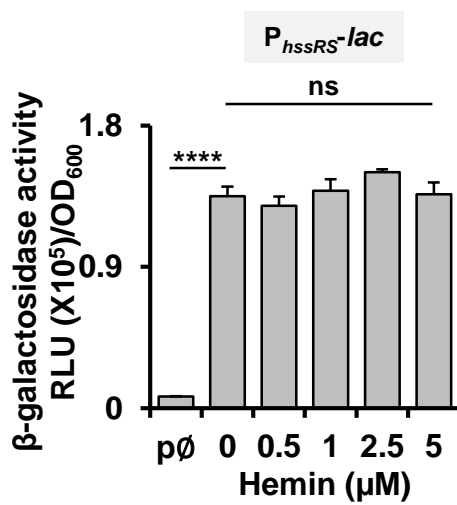
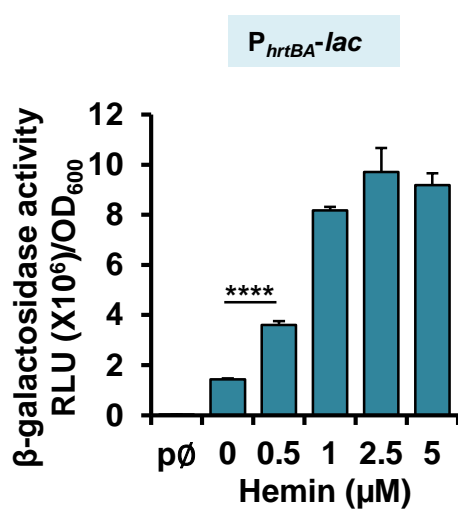
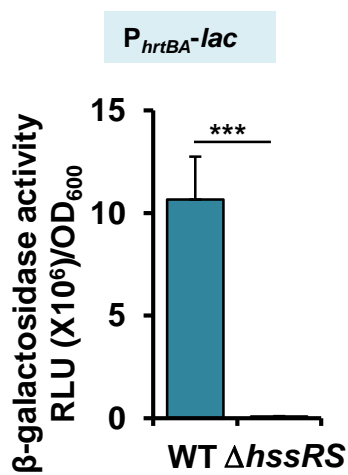
Membrane heme activates HssS

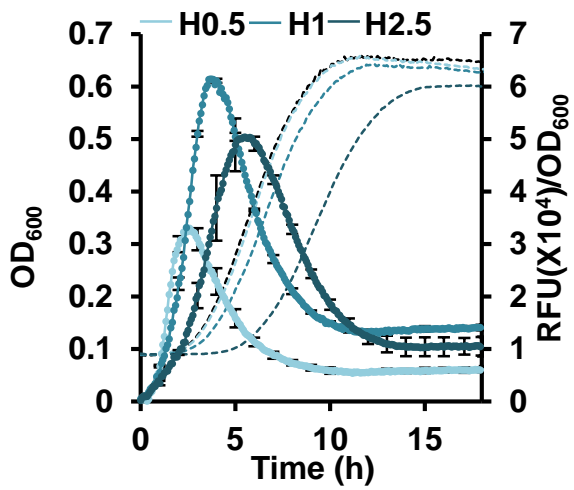
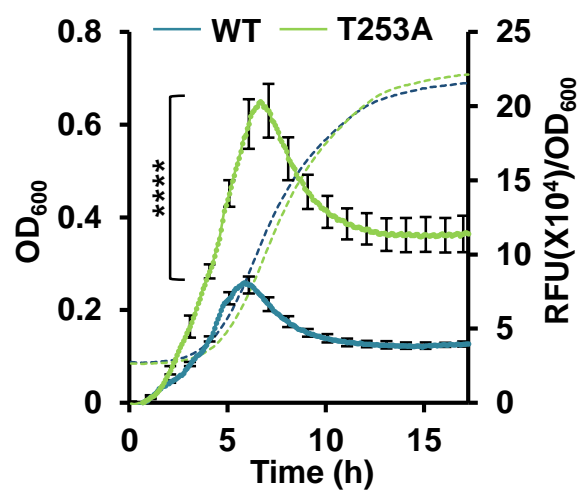
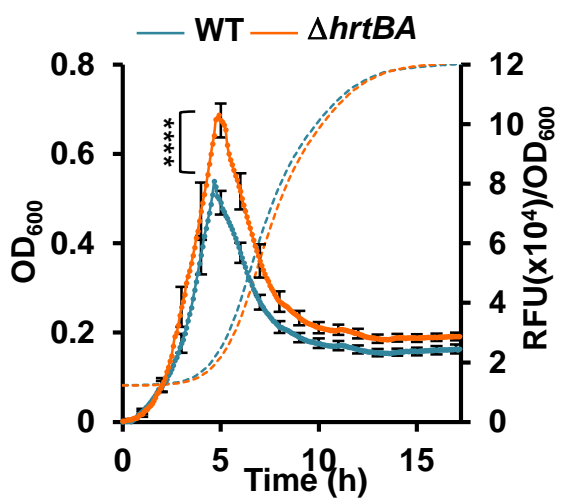
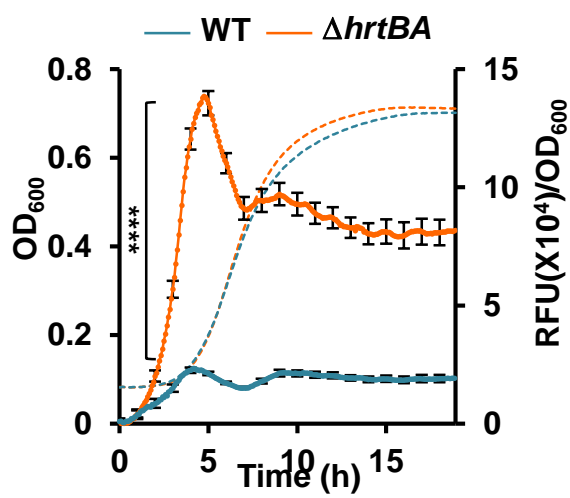
832 pGFP(HssS Δ ECD) or empty vector (p \emptyset). Bacteria were diluted from ON cultures to an
833 OD₆₀₀ = 0.01 and grown in BHI without (B) or with 10 μ M hemin in a microplate
834 spectrophotometer (Spark, Tecan). OD₆₀₀ was recorded every 15 min for the indicated time.
835 Results of bacterial growth minus medium background are displayed. Results represent the
836 average \pm S.D from triplicate biological samples.

837

838

839

A**B****C****D****Figure 1**

A**B****C****D****Figure 2**

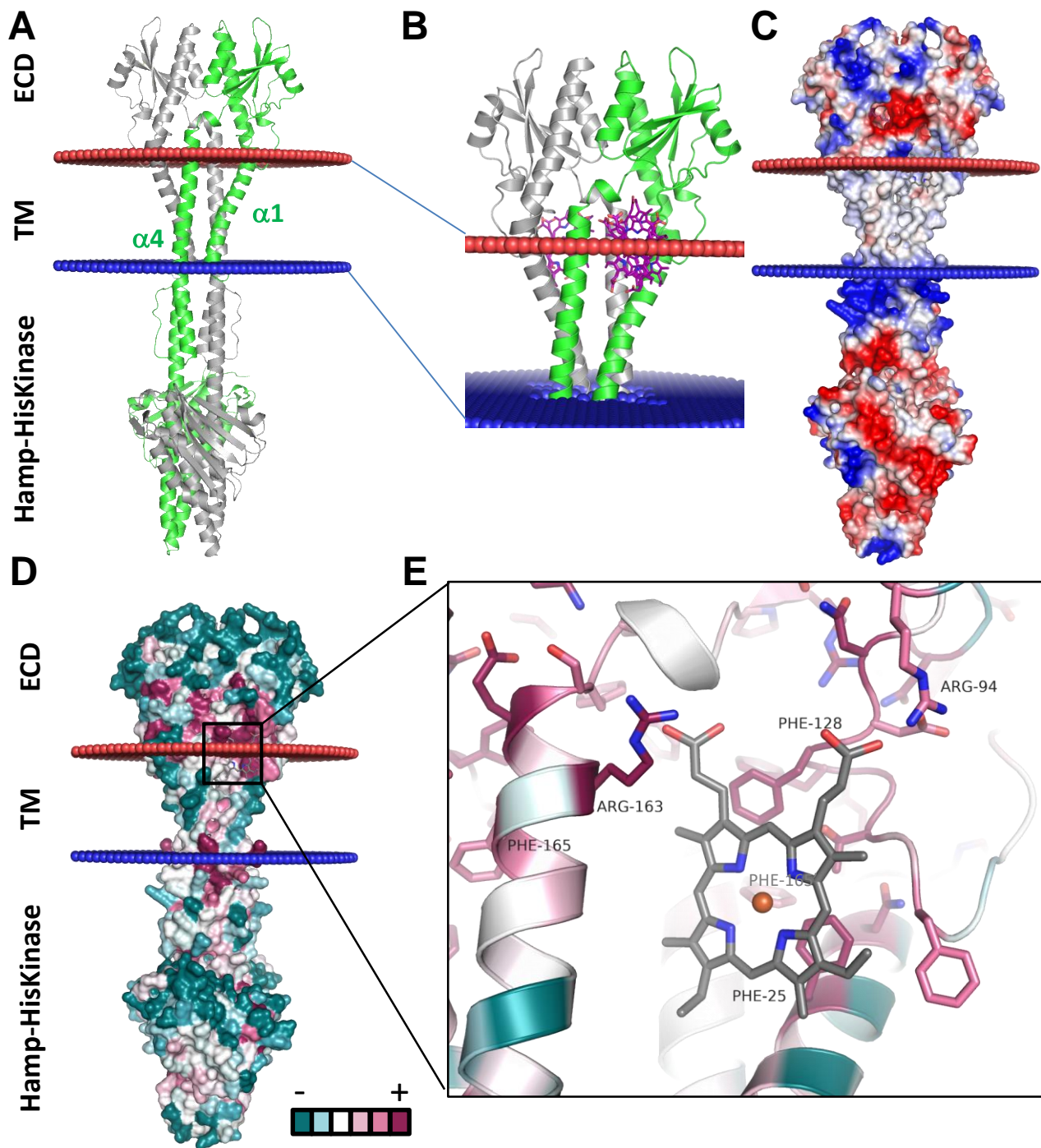


Figure 3

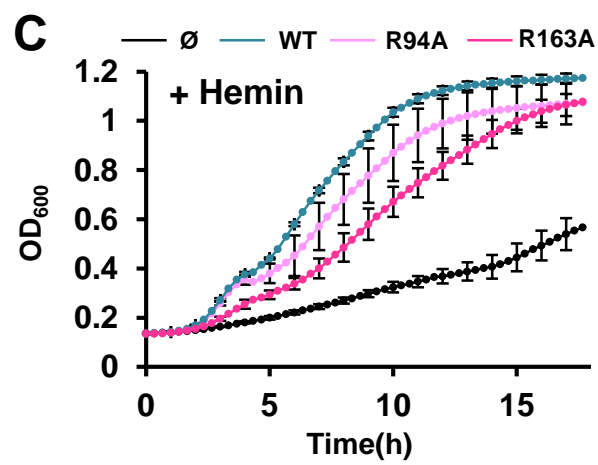
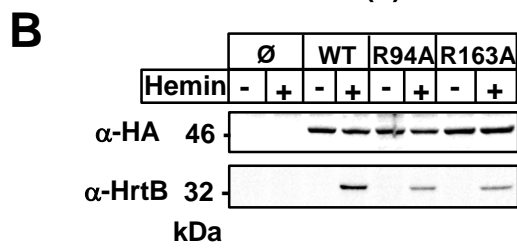
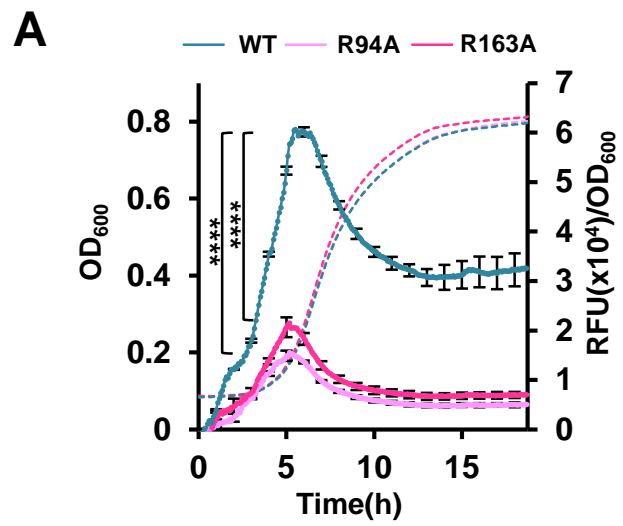


Figure 4

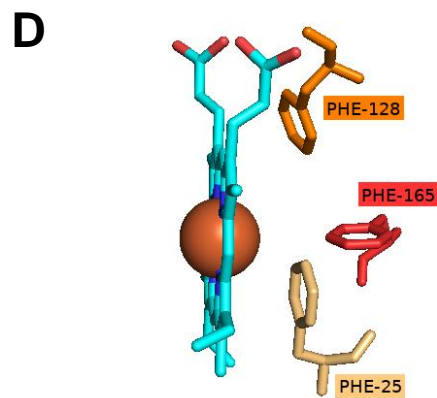
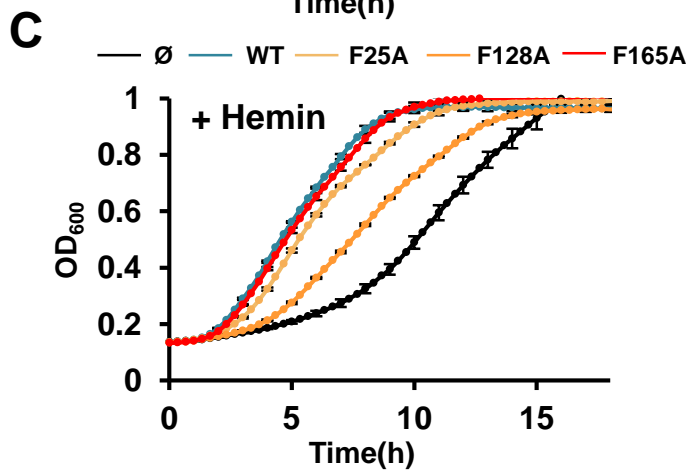
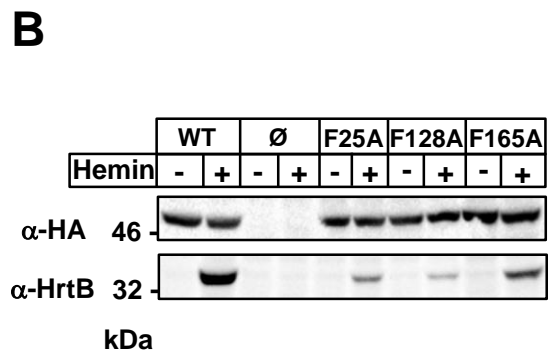
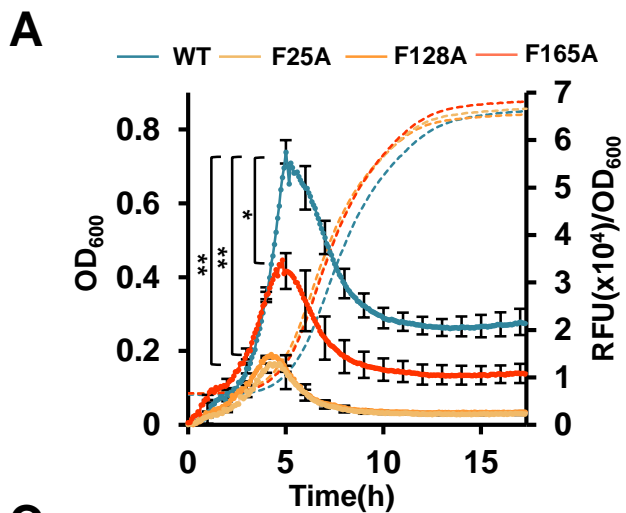


Figure 5

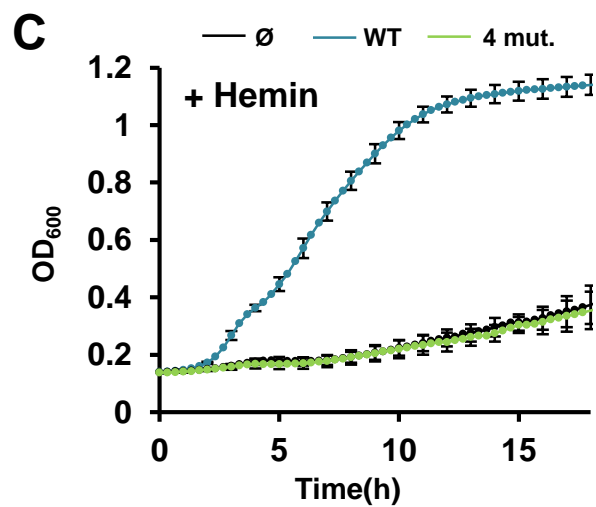
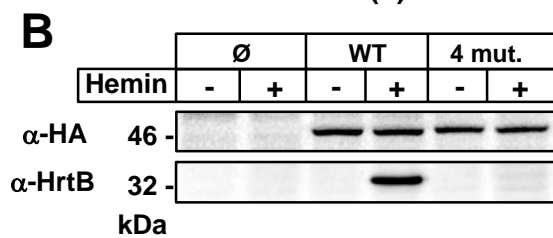
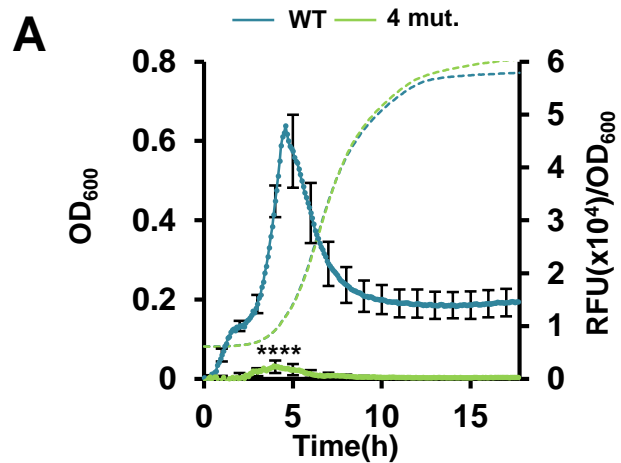


Figure 6

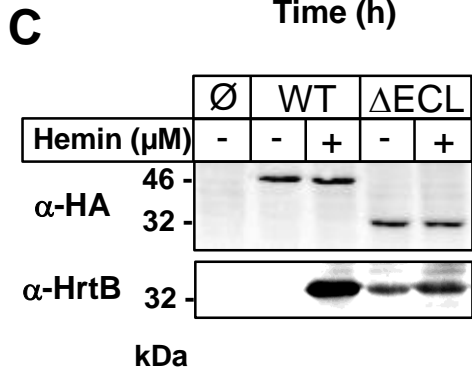
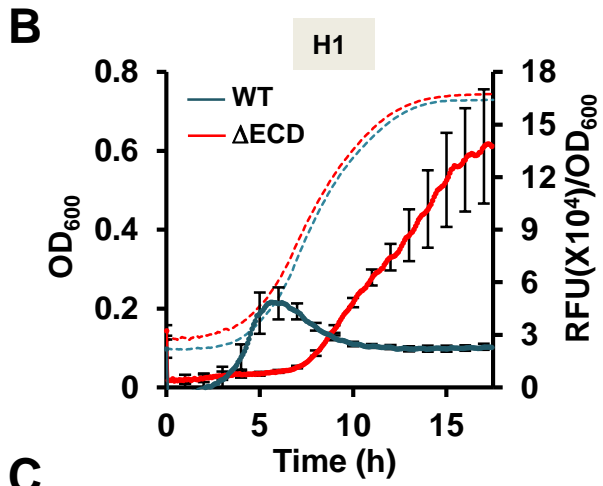
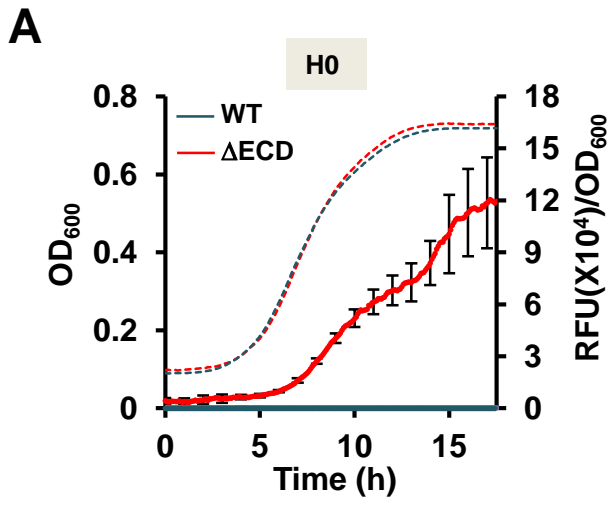


Figure 7

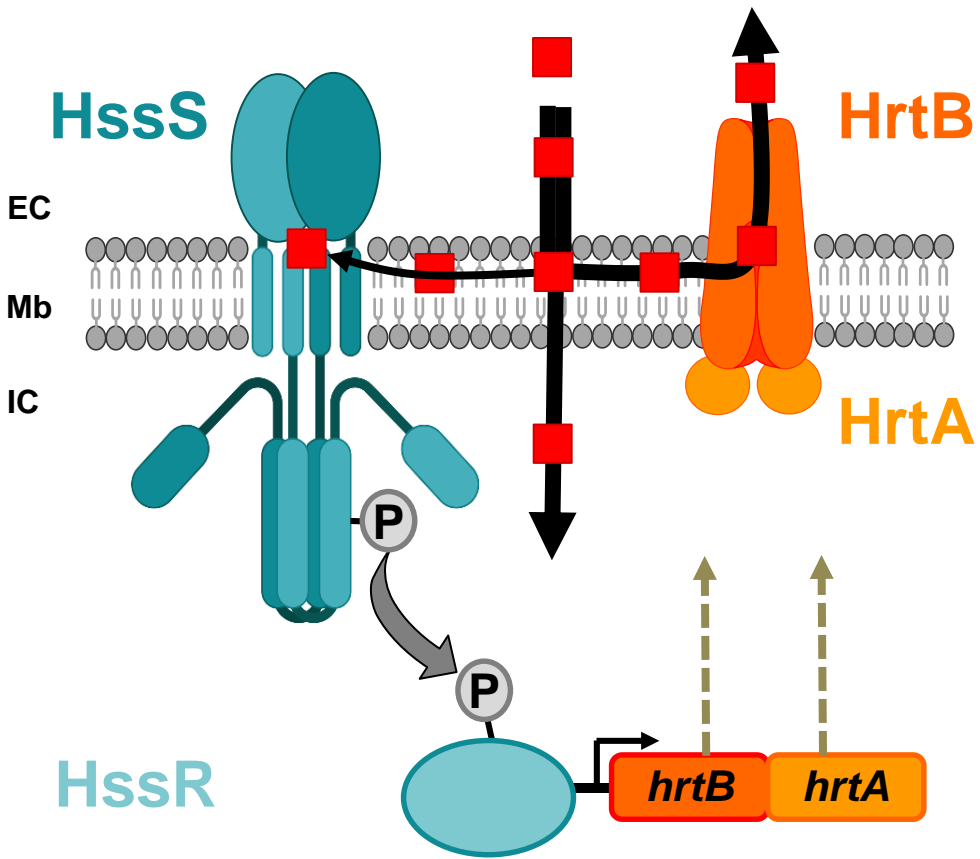


Figure 8

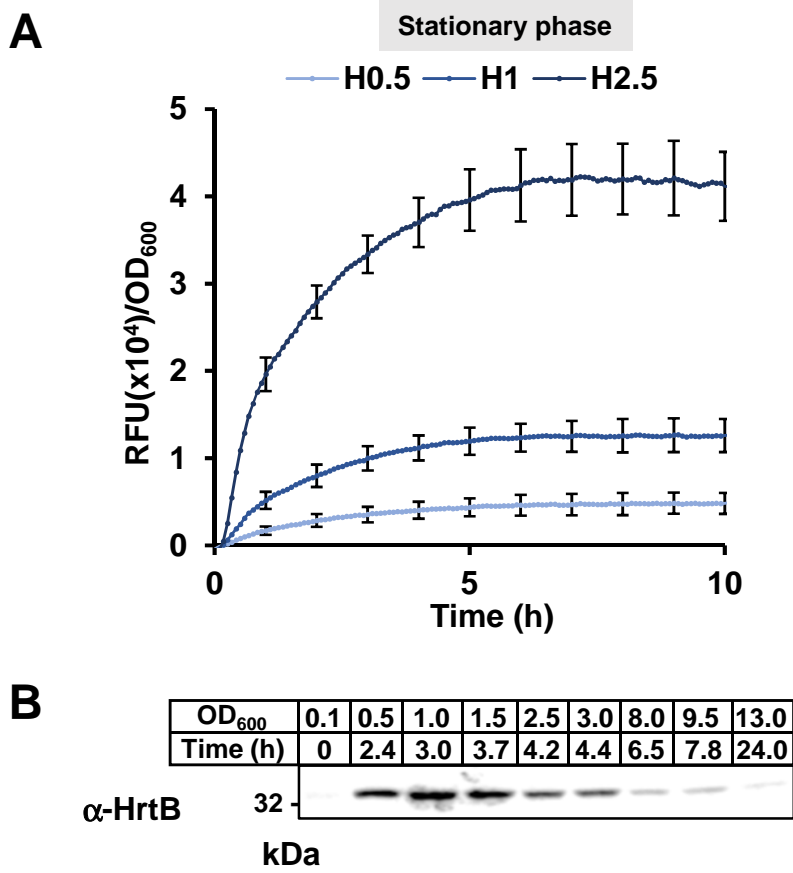
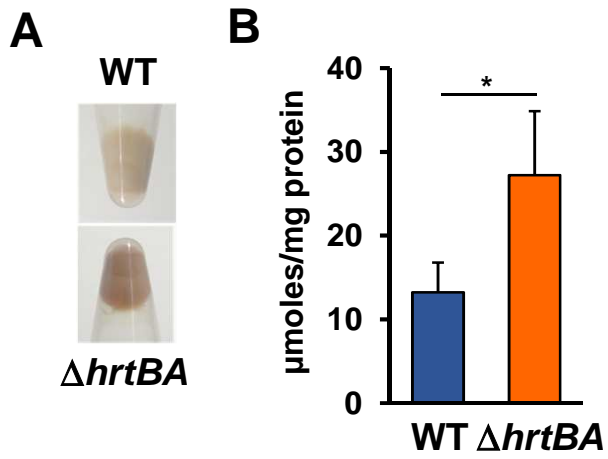


Figure S1



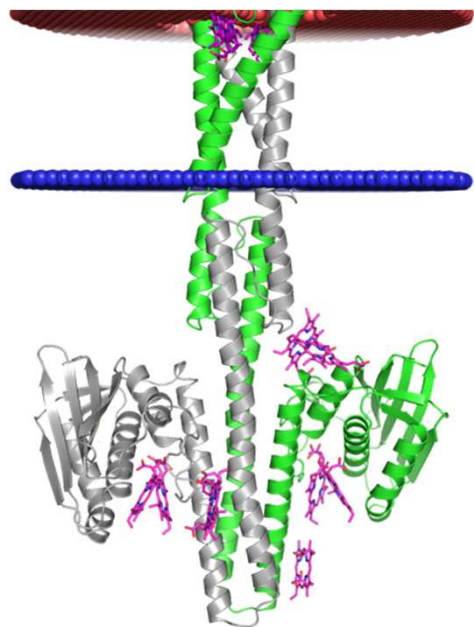


Figure S3

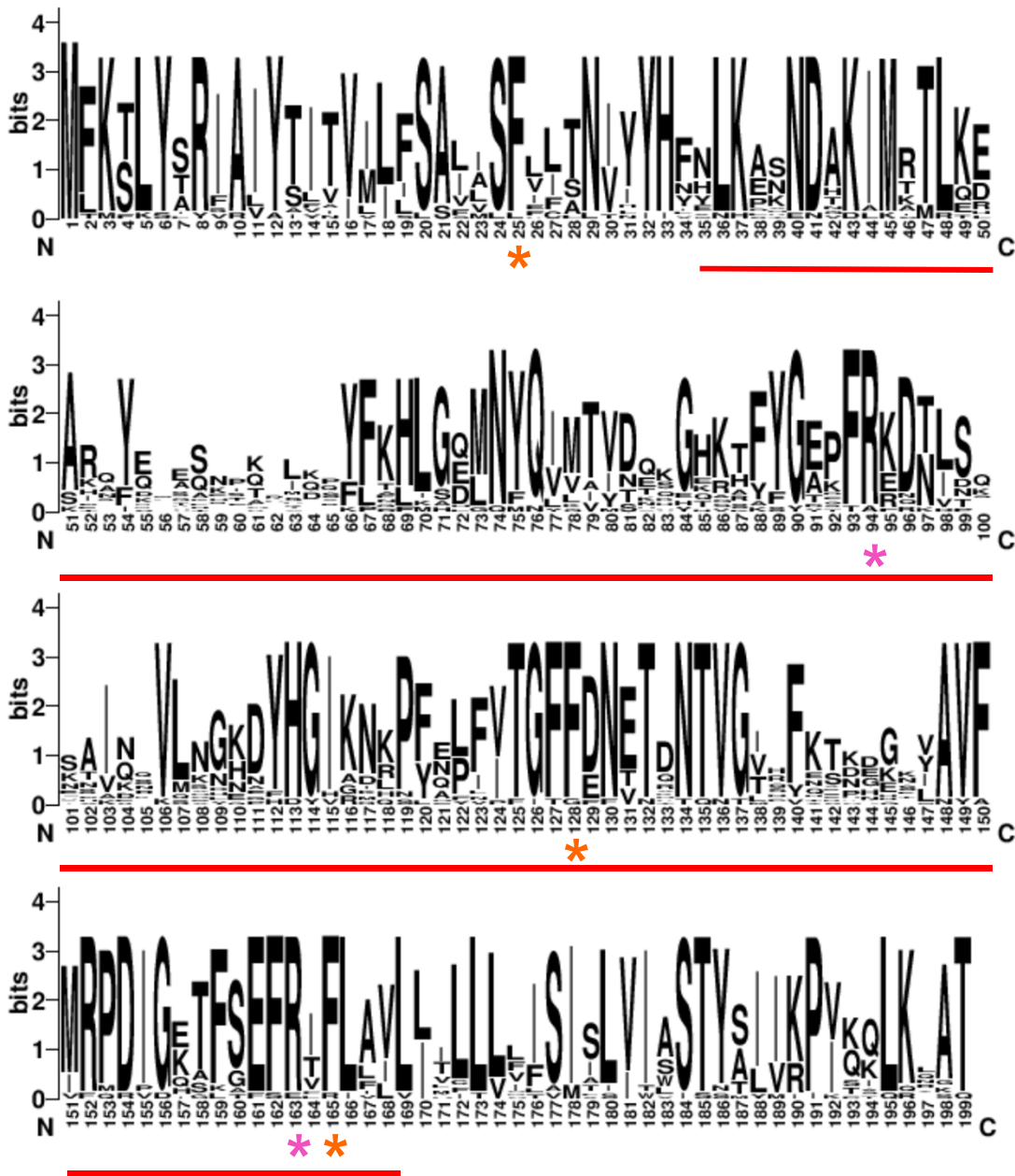


Figure S4

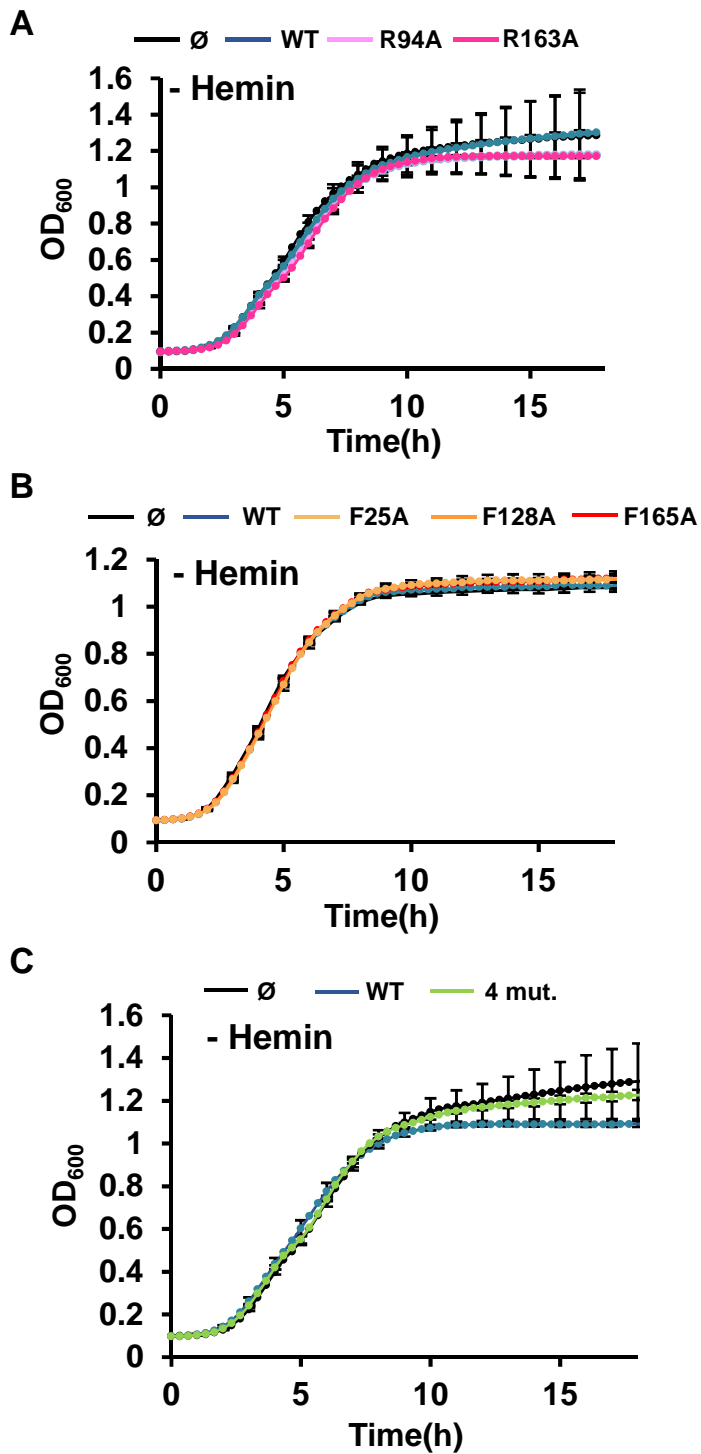


Figure S5

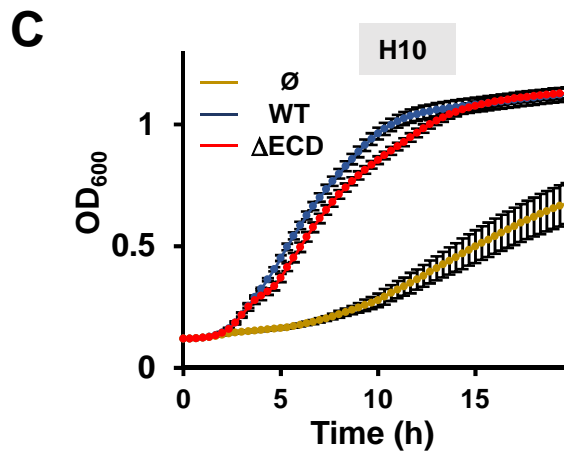
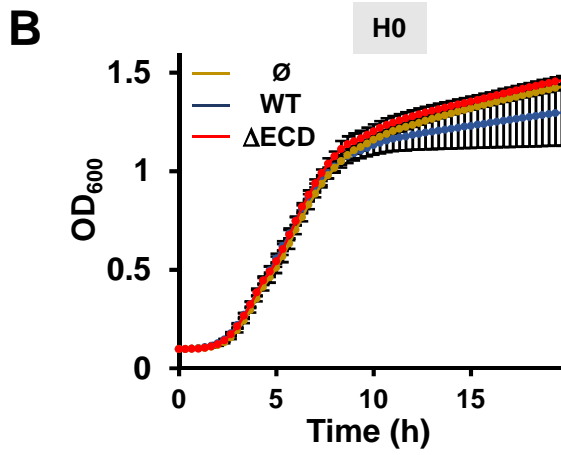
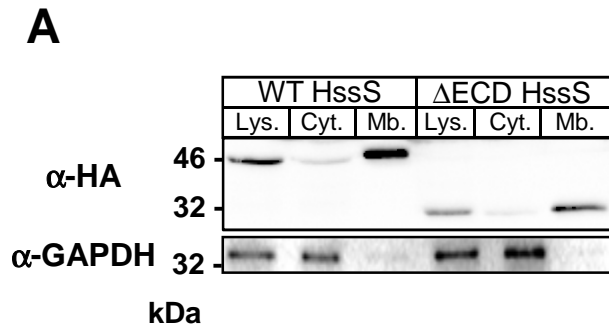


Figure S6